ANALYSIS OF SURFACE COMPOSITION AND CONTAMINANTS IN BIOLOGICAL SAMPLES BY HEAVY ION SCATTERING

by 6408

JON KENNETH WEST

B. S., Ottawa University, 1969

A MASTER'S THESIS

submitted in partial fulfillment of the

requirements for the degree

MASTER OF SCIENCE

Department of Physics

KANSAS STATE UNIVERSITY
Manhattan, Kansas

1971

Approved by:

JJ JJ Seaman
Major Professor

TABLE OF CONTENTS

INTRODUCTION

This paper presents a method to quantitatively, as well as qualitatively, determine contaminants in biological samples. The technique described below was applied to flour samples made from corn, wheat, and milo in order to determine if lead or mercury were present.

Biological samples are composed primarily of hydrogen, carbon, nitrogen, and oxygen. These elements alone make up most of the atoms in proteins[1] and carbohydrates.[2] Oxygen ions incident on such materials can not scatter into angles greater than 90° in the laboratory frame of reference.

This can best be visualized by considering the process of elastic scattering. The kinetic energy and the momentum of the system is conserved for elastic scattering. In the laboratory reference frame M_1, the incident particle, collides with M_2, the target particle which is at rest. In the center of mass reference frame both particles have the same speed and are traveling toward each other. The incident particle scatters into and angle θ with respect to the incident direction and retain their original speed in that direction. From the above considerations, the relations between laboratory and center of mass velocities can be found. Figure 1 shows the geometrical relation between laboratory

---

1. "Proteins," The Encyclopedia Americana, 1949 ed., XXII, p. 676.

2. Ferris, "Carbohydrate," The Encyclopedia Americana, 1949 ed., V, p. 587.

scattering and center of mass scattering;

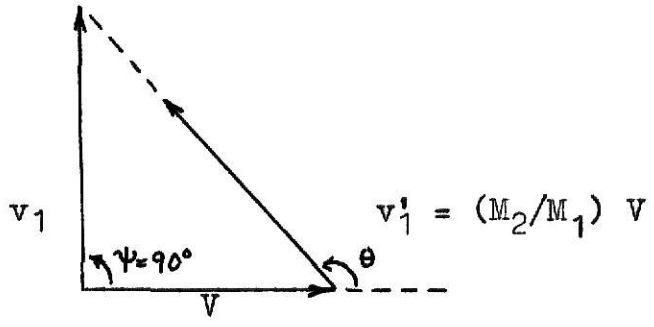

Fig. 1

where Ψ = laboratory scattering angle

θ = center of mass scattering angle

V = center of mass velocity before scattering

v_1 = laboratory velocity of incident particle, M_1, after scattering

v_1' = center of mass velocity of incident particle, M_1, after scattering

M_1 = incident particle mass

M_2 = target particle mass

From the figure it can be seen that v_1' is less than V for all cases where M_2 is less than M_1. In any real scattering situation the triangle must close. That is for Ψ greater than or equal to 90°, v_1' must be greater than V, the base of the triangle. This is true if and only if M_2 is greater than M_1.

M_1 is the oxygen ion and M_2 is either a contaminant or the flour. Oxygen is heavier than the atoms that form the carbohydrates and the proteins in flour. Therefore, Ψ in this will always be less than 90°. But, for contaminants heavier than oxygen, Ψ can be greater than 90°. Therefore, any massive atoms

such as lead or mercury will scatter the oxygen ions backwards while the flour itself will not. By detecting the backscattered oxygen ions and plotting the number of particles against the energy of the backscattered particle, the amount of a particular contaminant and its identity could be determined.

KINEMATICS OF ELASTIC SCATTERING FROM AN INFINITELY THICK TARGET

An oxygen beam of energy, E_o, incident on an infinitely thick target has an energy, E_o', at the time of elastic scattering as shown in plate I. The difference between the incident energy E_o and E_o' is ΔE_o and is due to the energy loss over the range of travel of the oxygen ions before elastic scattering. The scattered oxygen, M_1, has an energy, E_1', which becomes E_1 due to energy loss $\Delta E_1'$ as it exits from the target.

If the oxygen ion is scattered from the surface of the target, the scattered energy, E_1, becomes a maximum. This is true because there is no energy loss in that process.

From conservation of momentum and energy for elastic scattering, the ratio of E_1/E_0 is given by:

$$\frac{E_1}{E_0} = \frac{M_1^2}{(M_1+M_2)^2}\left\{\cos\Psi \pm \left[\left(\frac{M_2}{M_1}\right)^2 - \sin\Psi\right]^{\frac{1}{2}}\right\}^2$$

where the "+" sign is used unless M_1 is greater than M_2. Two simple cases are for $\Psi = 180^o$

$$E_1/E_0 = (M_1 - M_2)^2/(M_1 + M_2)^2$$

for $\Psi = 90^o$

$$E_1/E_0 = (M_2 - M_1)/(M_1 + M_2)$$

Plate II shows the ratio E_1/E_0 as a function of the laboratory scattering angle Ψ. For nuclear masses less than or equal to that of ^{16}O the ratio becomes zero for Ψ equal to or greater than 90^o. For nuclear masses heavier than ^{16}O the ratio has a finite value for all angles up through 180^o. Plate II shows that oxygen ions will only scatter into angles greater than

EXPLANATION OF PLATE I

Plate I A schematic drawing of the kinematics of elastic scattering from a thick target.

THIS BOOK CONTAINS NUMEROUS PAGES WITH DIAGRAMS THAT ARE CROOKED COMPARED TO THE REST OF THE INFORMATION ON THE PAGE.

THIS IS AS RECEIVED FROM CUSTOMER.

PLATE I

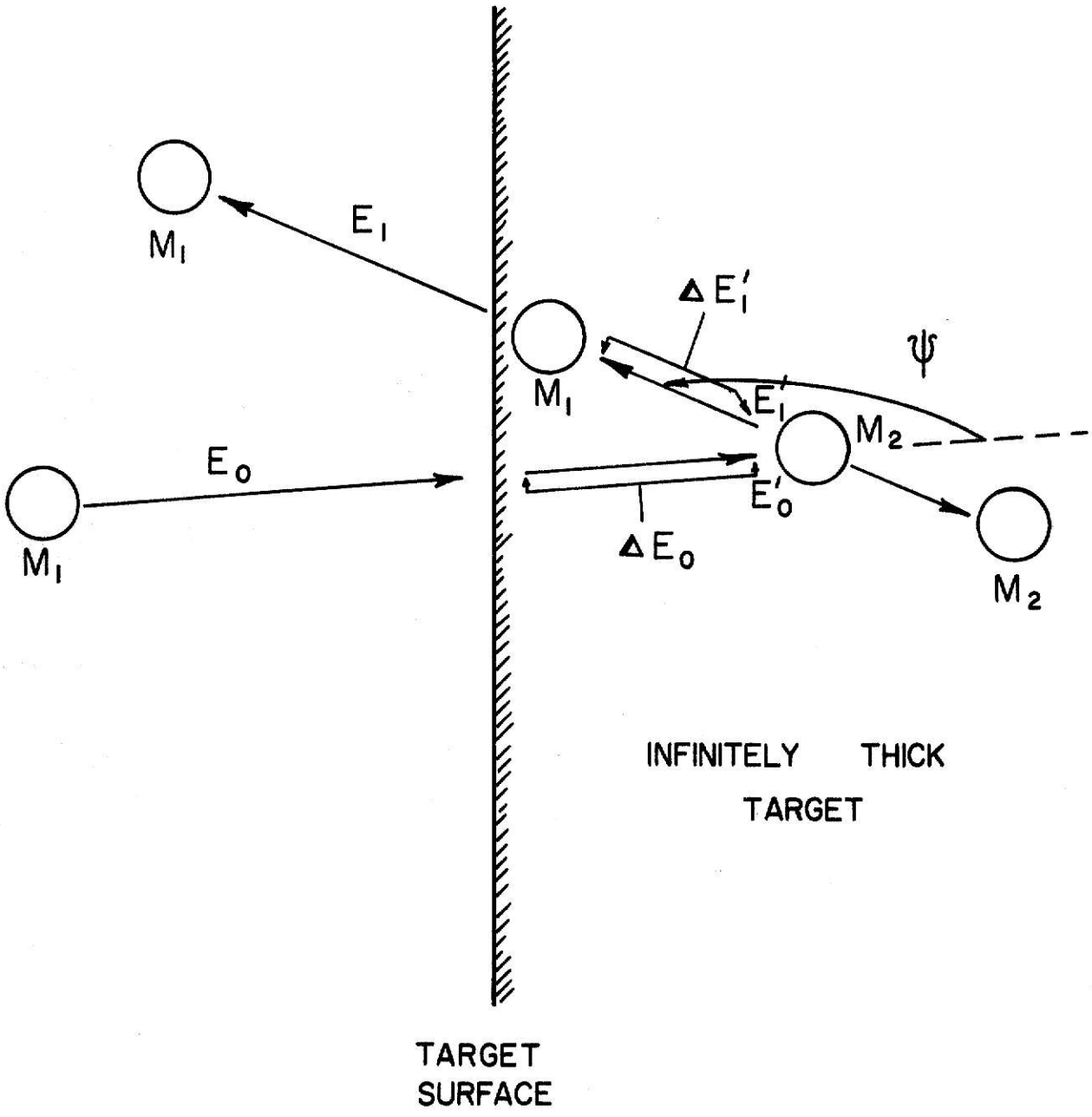
M1
E1
M1
ΔE1'
ψ
E1'
M2
E0
M1
E0'
ΔE0
M2
INFINITELY THICK
TARGET
TARGET
SURFACE

90^{o} for target masses greater than ^{16}O.

The above arguments give a means of determining the nuclear mass from which the incident oxygen ions are scattered. The maximum energy of the backscattered oxygen ion determines the heaviest contaminant in the flour sample. In order to determine the amount of this contaminant, the number of particles scattered into a particular solid angle must be known.

The particle yield, Y, from a thin target is given by the following expression.[3]

$$Y\,dx = N_o\, n\, \frac{d\sigma}{d\Omega}\, \Delta\Omega$$

where N_o = number of incident ions

n = number of target atoms per cm^2

$\Delta\Omega$ = solid angle subtended by the detector

$\frac{d\sigma}{d\Omega}$ = differential cross section per unit solid angle

In order to calculate the total particle yield from a thick target, the sum of successive thin target particle yields must be taken.

$$\int Y\,dx = N_o\, n\, \Delta\Omega \int \frac{d\sigma}{d\Omega}\, \frac{dE}{dE/d(\rho x)}$$

A program was written to calculate this total yield and sample calculations are tabulated in a later section.

The Rutherford differential cross section is defined as

---

3. Leighton, Principles of Modern Physics, p. 490.

EXPLANATION OF PLATE II

Plate II A graph of E_1/E_0 as a function of the laboratory angle ψ for several different target nuclei.

PLATE II

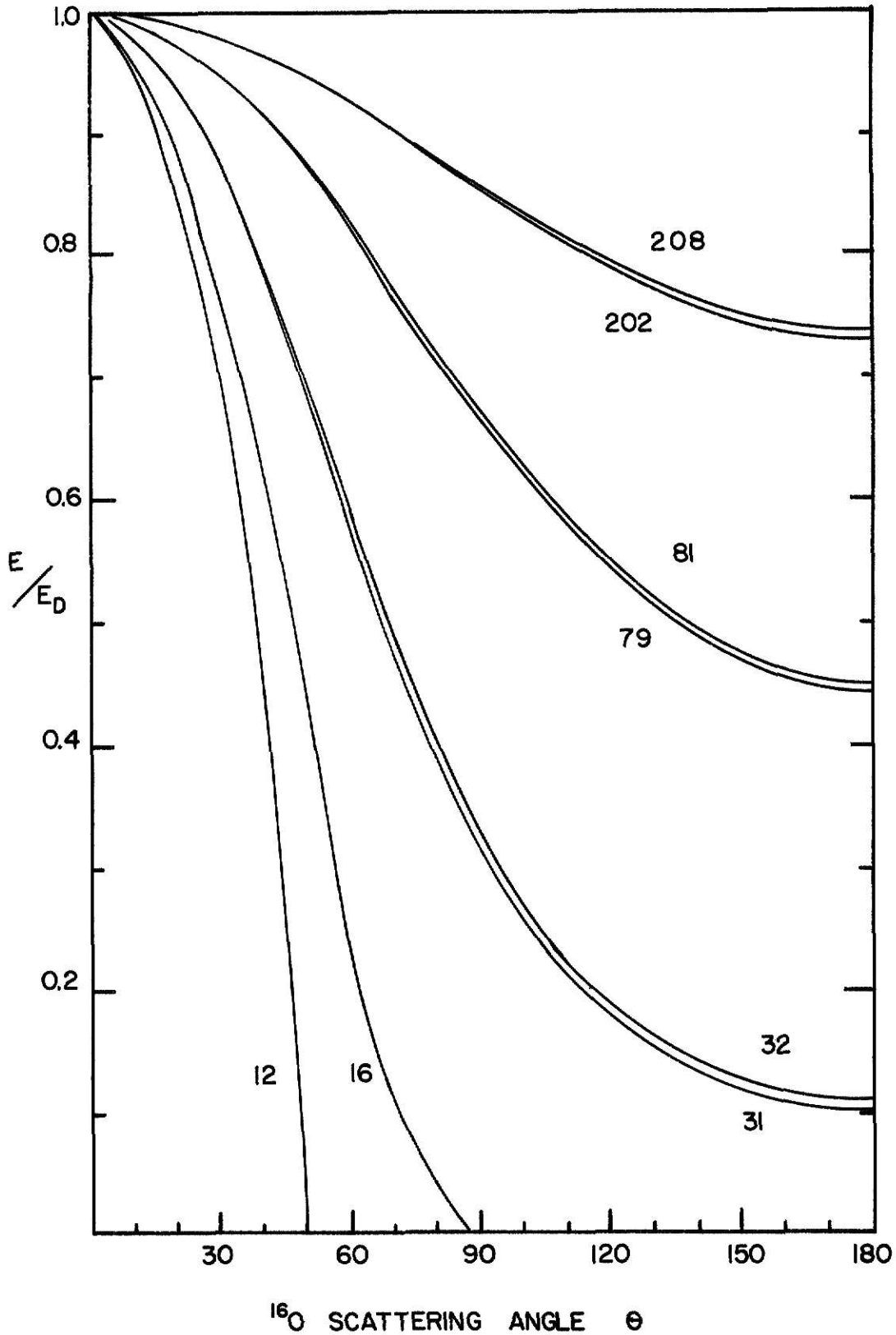
1.0
0.8
0.6
0.4
0.2
E/E_D
208
202
81
79
32
31
16
12
30
60
90
120
150
180
16O SCATTERING ANGLE θ

the collision area effective for producing scattering into a unit solid angle for a particular angle θ_{cm}, where the angle θ_{cm} is the scattering angle in the center of mass system.

The Rutherford differential cross section[4] per unit solid angle, $\frac{d\sigma}{d\Omega}$, is given by

$$\frac{d\sigma}{d\Omega} = \frac{e^4 Z_1^2 Z_2^2}{16 E_0^2 \sin^4\left(\frac{\theta_{cm}}{2}\right)}$$

where E_0 = the incident particle energy

Z_1 = the atomic number of the incident particle

Z_2 = the atomic number of the target particle

θ_{cm} = the center of mass scattering angle

In order to convert from the center of mass system to the laboratory system, $d\Omega(\theta)_{cm}$ is given in terms of $d\Omega(\psi)$.

$$\frac{d\Omega(\psi)}{d\Omega(\theta)_{cm}} = \frac{M_1 M_2}{(M_1+M_2)^2} \frac{\left[\left(\frac{M_2}{M_1}\right)^2 - \sin^2\psi\right]^{1/2}}{\left(E_1/E_0\right)}$$

Also, the center of mass angle θ_{cm} is given in terms of ψ.

$$\theta_{cm} = \psi + \sin^{-1}\left(\frac{M_1}{M_2}\sin\psi\right)$$

Because the energy loss for the ^{16}O ion in flour is needed to calculate the thick target yield, this is the next process to consider.

The most significant contribution to the energy loss process is due to ionization. As a fast moving charged particle passes near or through an atom, it interacts with the orbital

---

4. French, Principles of Modern Physics, p. 332.

electrons as well as atomic nucleus. In this process an electron is occasionally given sufficient energy to escape from the atom to which it is bound. This energy is acquired at the expense of the fast moving incident particle, with the result that the moving particle is decelerated and may gradually be brought to rest. Electrons ejected directly from the atom by ionization may have energies up to $4m_eE_o/M$, which is about 0.002 E_o of the initial energy of the ionizing (incident) particle.[5]

There are also radiation energy losses for energetic particles. They are Bremsstrahlung or braking radiation and Cerenkov radiation or radiation due to particle velocities above the velocity of light in that particular medium. For example, the ratio of particle velocity to the speed of light, v/c, for 30 MeV oxygen is approximately 0.0635. Therefore, the most energetic particles used in this method were clearly non-relativistic. These processes can be neglected for oxygen ion of energies below 30 MeV.[6]

"Range and Stopping-Power Tables for Heavy Ions," by Northcliffe and Schilling,[7] was used to determine the stopping-power of oxygen ions in flour samples. As stated before, the major constituents of flour samples are oxygen, carbon, nitrogen, and hydrogen. Carbohydrates have a general chemical formula

---

5. Paul, Nuclear and Particle Physics, pp. 99-100.

6. Paul, loc. cit.

7. Northcliffe and Schilling, "Range and Stopping-Power Tables for Heavy Ions," Nuclear Data Tables, p. 268.

$C_{6n}H_{2p}O_p$.[8] For proteins, carbon is present in amounts varying from 50 to 55 percent, hydrogen from 6.9 to 7.2 percent, oxygen from 19 to 24 percent, nitrogen from 18 to 19 percent, and sulfur from 0.3 to 2.4 percent.[9] Plate III shows a graph of dE/dx as a function of energy E_o. The difference between polyethylene and water is slight. The plate also shows the approximation used for flour which is bracketed by $(CH_2)_n$ and H_2O.

---

8. Ferris, loc. cit.

9. "Proteins," The Encyclopedia Americana, loc. cit.

EXPLANATION OF PLATE III

Plate III A graph of stopping-power dE/dx as a function of the incident energy E_o for several organic compounds as well as the approximation used for flour.

PLATE III

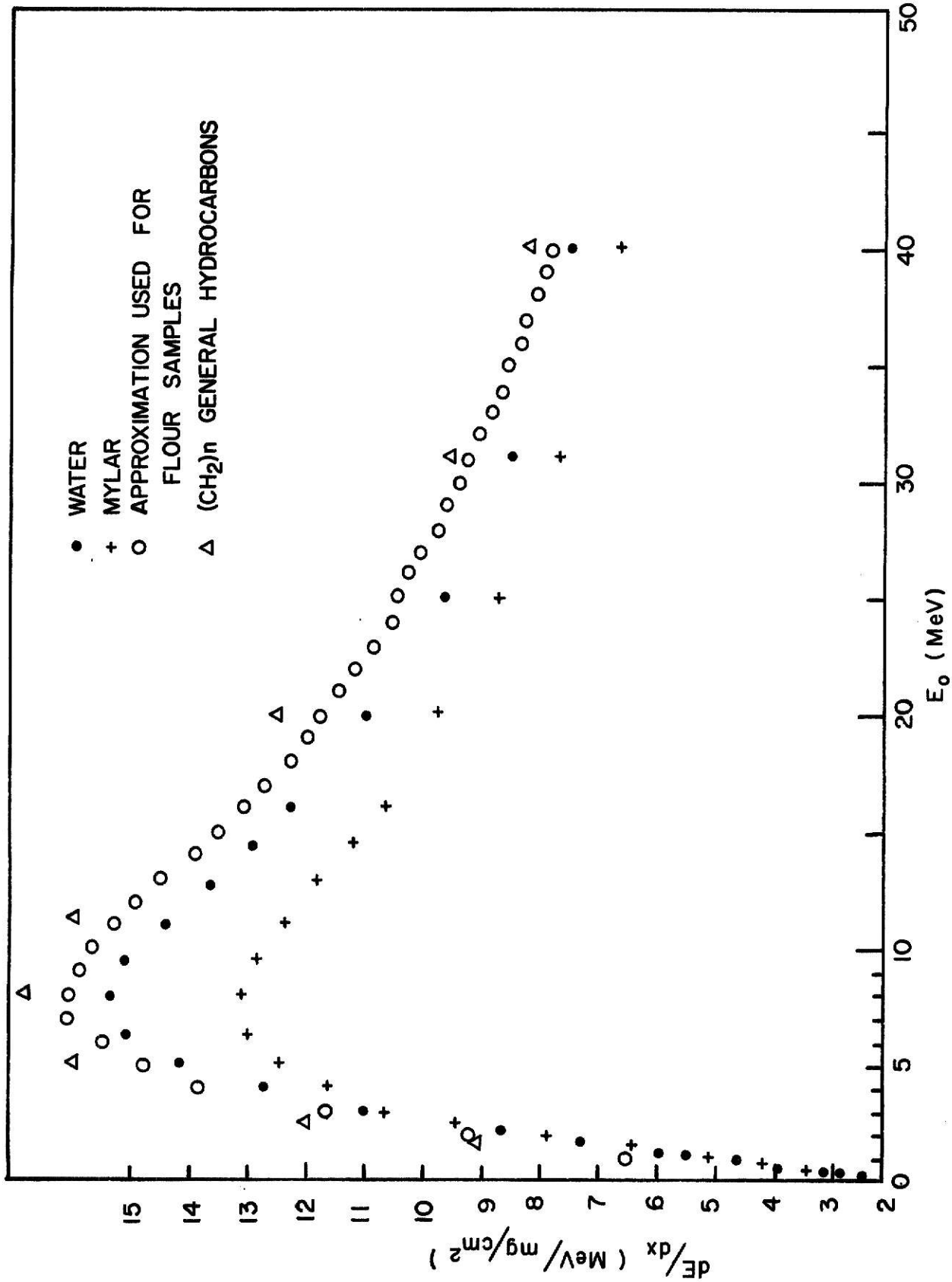
WATER
MYLAR
APPROXIMATION USED FOR FLOUR SAMPLES
(CH2)n GENERAL HYDROCARBONS
dE/dx (MeV/ mg/cm2)
E0 (MeV)
0
5
10
20
30
40
50
2
3
4
5
6
7
8
9
10
11
12
13
14
15

EXPERIMENTAL PROCEDURE

Initially flour samples were simply mixed with distilled water and allowed to dry on aluminum target holders. Targets that were incompletely dried created several problems. It was very difficult to pump the chamber down with "wet" targets and the vacuum became much worse when the beam was allowed to hit the target. Also, spectra taken under such conditions could not be reproduced when the targets began to dry out. Although satisfactory spectra could be obtained from dry targets made in this manner, several samples fell from the holders under vacuum.

For calibration and identification purposes, small amounts of lead, bromine, and mercury were mixed with flour samples. Several spectra were obtained before a satisfactory method was developed to make these samples. Small masses of $PbNO_3$, $HgNO_3$, and KBr were dissolved in one liter of distilled water. Then one milliliter of the mixture was pipetted and mixed with a known mass of flour. The mixture was then allowed to dry. In the next step, the flour and the contaminant were powdered and mixed with a known mass of polystyrene dissolved in benzene. This mixture was allowed to dry under vacuum on aluminum target holders. Different masses of polystyrene were used in order to make the flour targets durable.

It was found that polystyrene in amounts greater than twenty percent of the total mass of the target gave unreliable spectra. As polystyrene is a good insulator, a positive charge builds up on the sample. A discharge results which causes high

level noise pulses in the particle detector at a high rate, thus distorting the spectrum.

The eight flour samples discribed below were made simply by using distilled water while all of the calibrated flour targets were produced using the polystyrene method.

Initially, only particles scattered between 165^{o} and 175^{o} from the incident direction were detected. A schematic of the target chamber used is shown in plate IV. In order to detect scattered particles at 90^{o}, the target chamber shown in plate V was used.

Accelerated beams of oxygen ions of charge states three, four, and five were obtained from the Kansas State University's Tandem Van de Graaff accelerator with energies from 12 to 30 MeV. The beam currents available varied with conditions of the source and overall machine conditioning. The currents on target ranged from one half nanoampere to several hundred nanoamperes.

The target current and total beam current were measured separately. The targets were removed from the beam and the ion current was measured in a faraday cup. The targets were then replaced and the current on the targets was measured. Because the charged particles incident upon the target ejected electrons, the measured target current was more than the true beam current. This was found to be true for the flour targets where the beam spot was smaller than the targets. This procedure was used as a check on all runs where the total yield was calculated.

A block diagram of the electronics used is shown in plate VI. Pulses from the detector were amplified with the

EXPLANATION OF PLATE IV

Plate IV A schematic drawing of the target chamber used to detect particles scattered into 180°.

PLATE IV

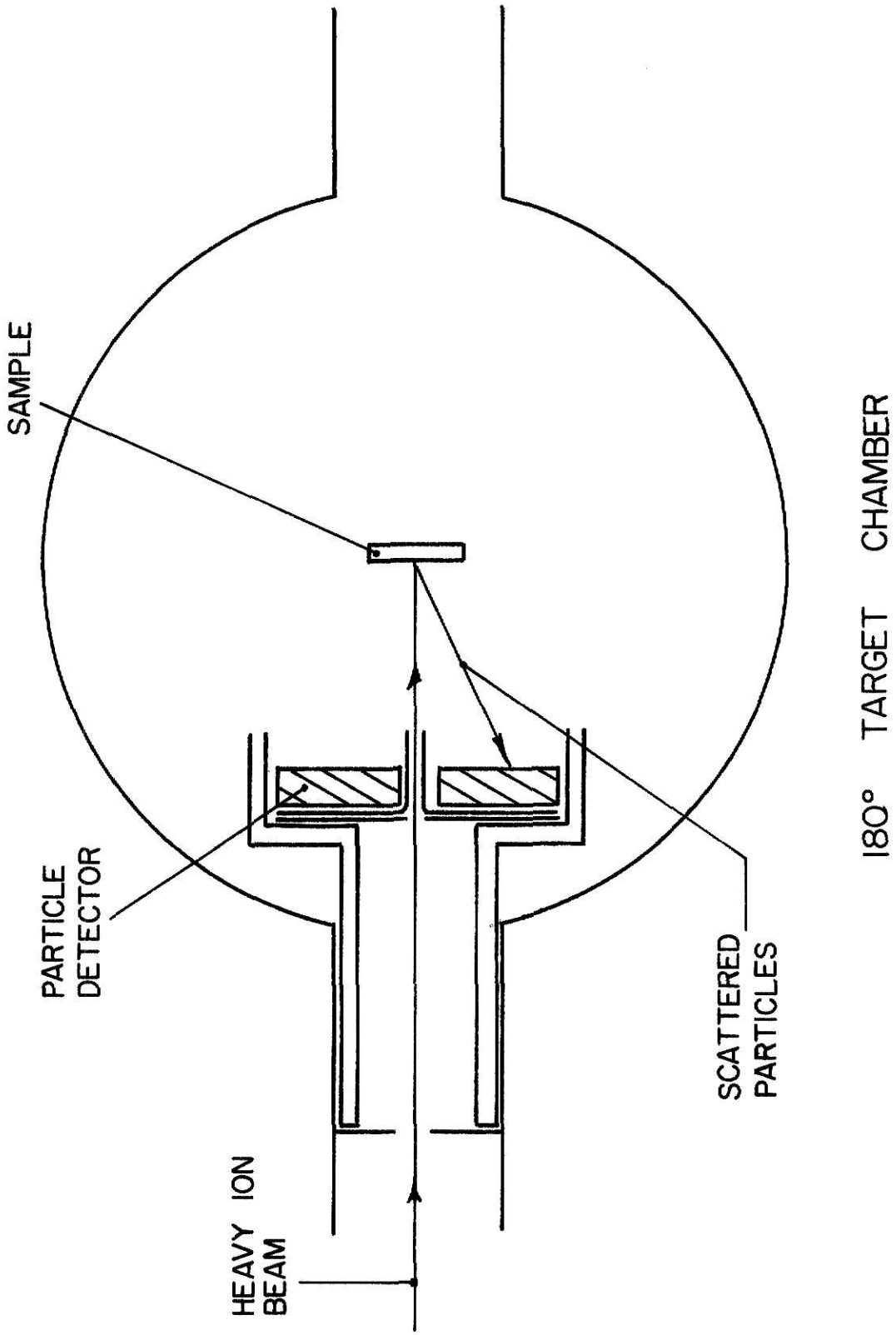
SAMPLE
PARTICLE DETECTOR
HEAVY ION BEAM
SCATTERED PARTICLES
180° TARGET CHAMBER

EXPLANATION OF PLATE V

Plate V A schematic drawing of the chamber used to detect particles scattered into 90^{o}.

PLATE V

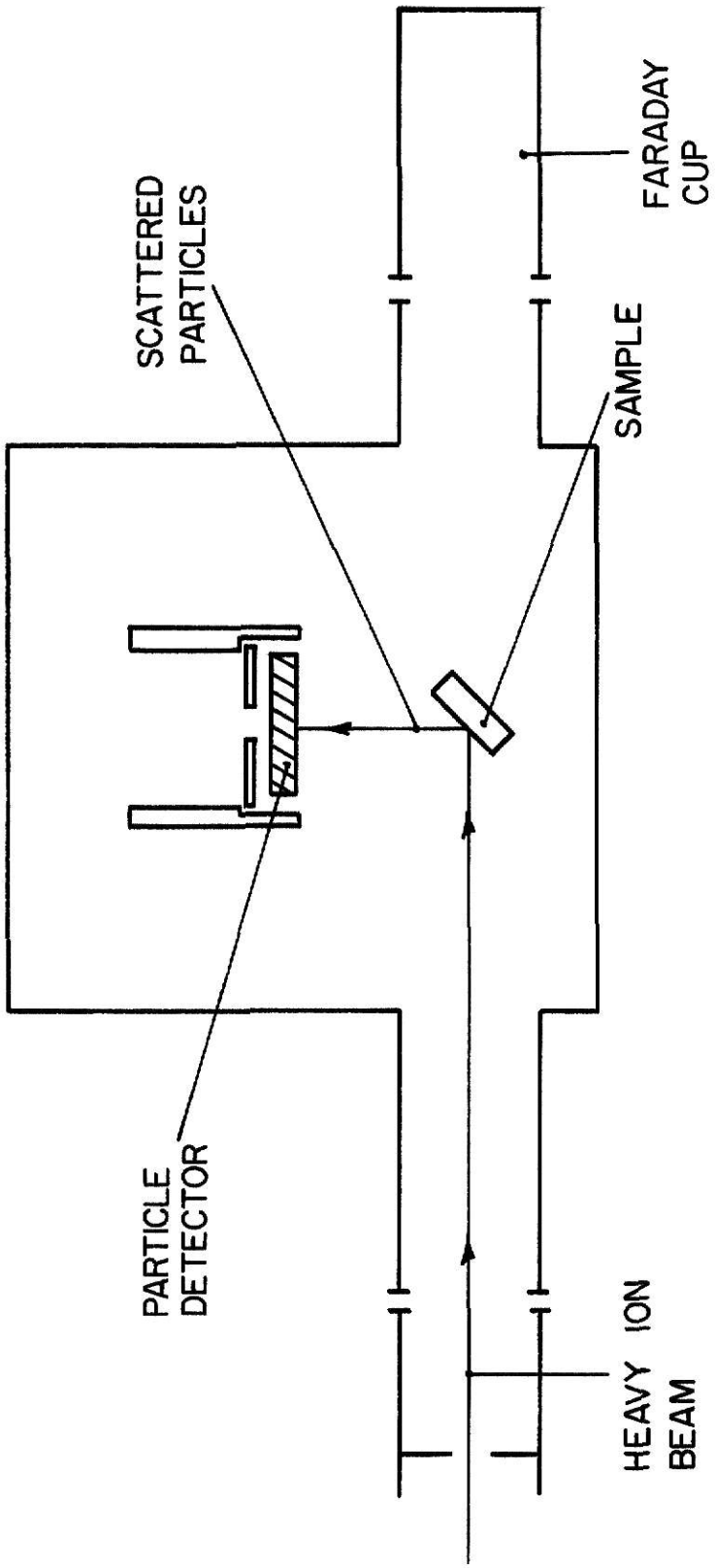

90° TARGET CHAMBER

EXPLANATION OF PLATE VI

Plate VI A schematic diagram of the electronic circuit used for integrating current runs.

PLATE VI

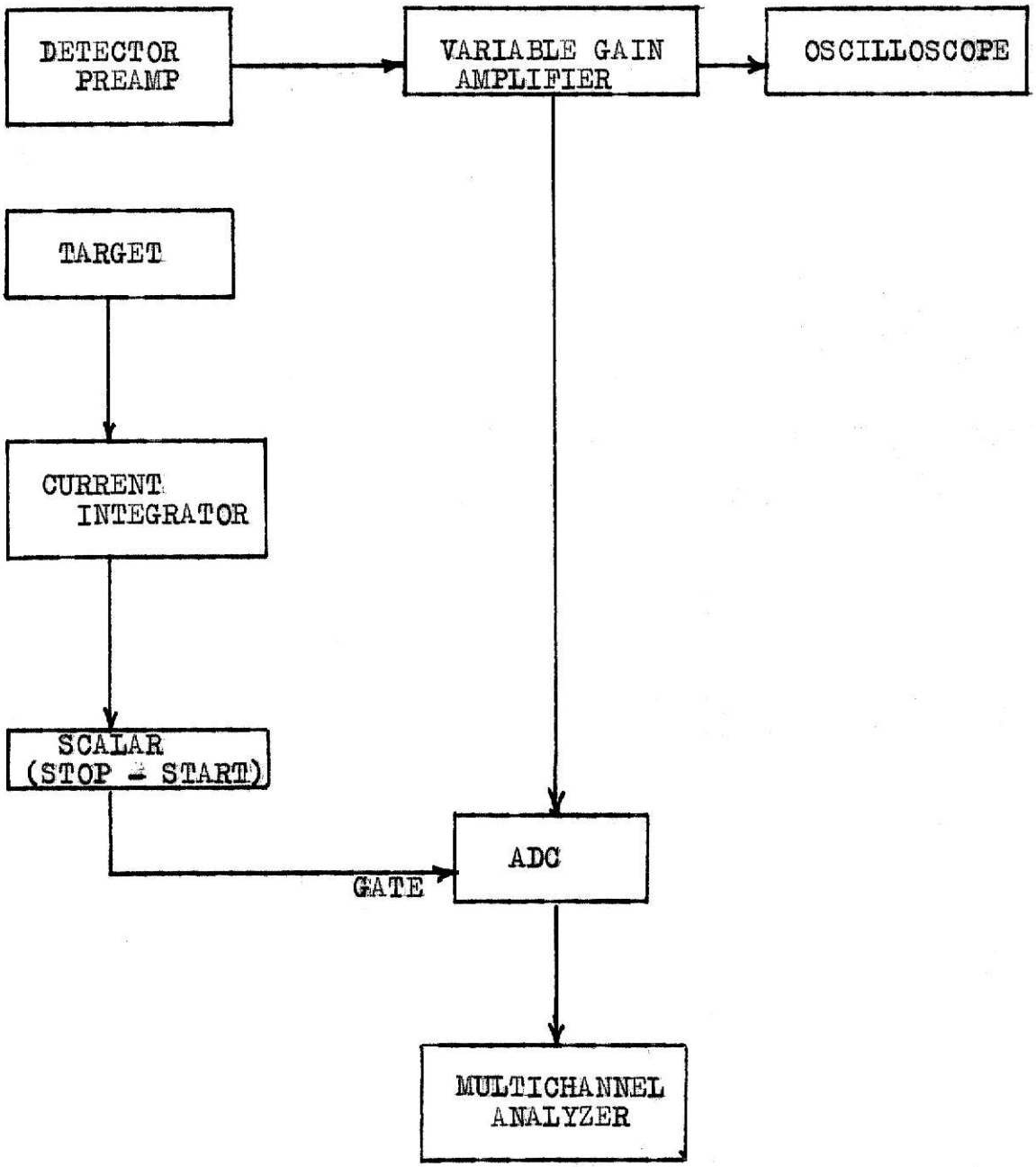
DETECTOR PREAMP
VARIABLE GAIN AMPLIFIER
OSCILLOSCOPE
TARGET
CURRENT INTEGRATOR
SCALAR (STOP - START)
GATE
ADC
MULTICHANNEL ANALYZER

appropriate gain in order to give a good spectrum for tantalum. The amplified pulse was then routed to the analog-to-digital converter (ADC) connected to a multichannel analyzer. The beam current incident on the target was collected in the integrator circuit, which gave a digital output proportional to the collected charge. A scalar recorded the number of counts from the current integrator. The ADC and scalar were both stopped and started simultaneously by gating the ADC with a DC level from the scalar which was +5 volts when the scalar was on and 0 volts when off.

SPECTRA OBTAINED AT 170° FROM 30 MEV, 24 MEV, AND 12 MEV ^{16}O IONS

Plates VII through XI are spectra obtained from ^{16}O scattered into 170° from different targets. Tantalum was used for calibration throughout the development of this method. A typical tantalum spectra for 24 MeV ^{16}O scattered into 170° is shown in plate VII. Since the energy does not vary strongly with angle near 180°, one can approximate the scattered energy expected by the formula for 180° scattering (see plate II). The following formula

$$E_1/E_0 = (M_1 - M_2)^2/(M_2 + M_1)^2$$

yields an energy ratio of 0.7021 for the "tantalum edge," and the exact calculation gives 0.7032.

After the tantalum edge was determined, the atomic mass of the target was plotted as a function of channel number. This curve was fitted to the channel number of the tantalum edge. This fitted curve is shown in plate VIII. Several different targets were used in order to verify this curve. Potassium and the bromine edges were plotted on the fitted curve. Aluminum targets were also used for 24 MeV ^{16}O ions. The results, shown in plate VIII, show good agreement with experimental data and the kinematic curve.

After the process was shown to be effective for targets made of a high concentration of a known element, a sample of flour was tried. Plate IX shows a spectrum for 24 MeV ^{16}O scattered into 170° from 100 ppm $PbNO_3$ in flour. As can be seen, there is a marked difference in the spectrum shape of the flour and tantalum.

In order to explain the spectra obtained, different incident energies were used. It was found that the spectrum shape was a function of incident energy. Plate X shows 12 MeV ^{16}O scattered into 170° from 100 ppm $PbNO_3$ in flour. At this energy the spectra very closely agreed with the shape of the tantalum spectrum. This was also true for different contaminants. For this spectrum the lead or mercury edge was detected and the energy of that edge agreed with the predicted energy.

Plates XIa and b show the same spectrum with different scales. Plate XIb shows a pure flour spectrum for 30 MeV ^{16}O scattered into 170°. This spectrum shape differs greatly from that of tantalum. Plate XIa shows a predicted spectrum for ^{207}Pb in flour superimposed on the pure flour spectrum. The predicted spectrum shape shows good agreement with the 12 MeV spectra and the initial spectra.

EXPLANATION OF PLATE VII

Plate VII Spectrum of 24 MeV ^{16}O scattered into 170° from ^{181}Ta.

PLATE VII

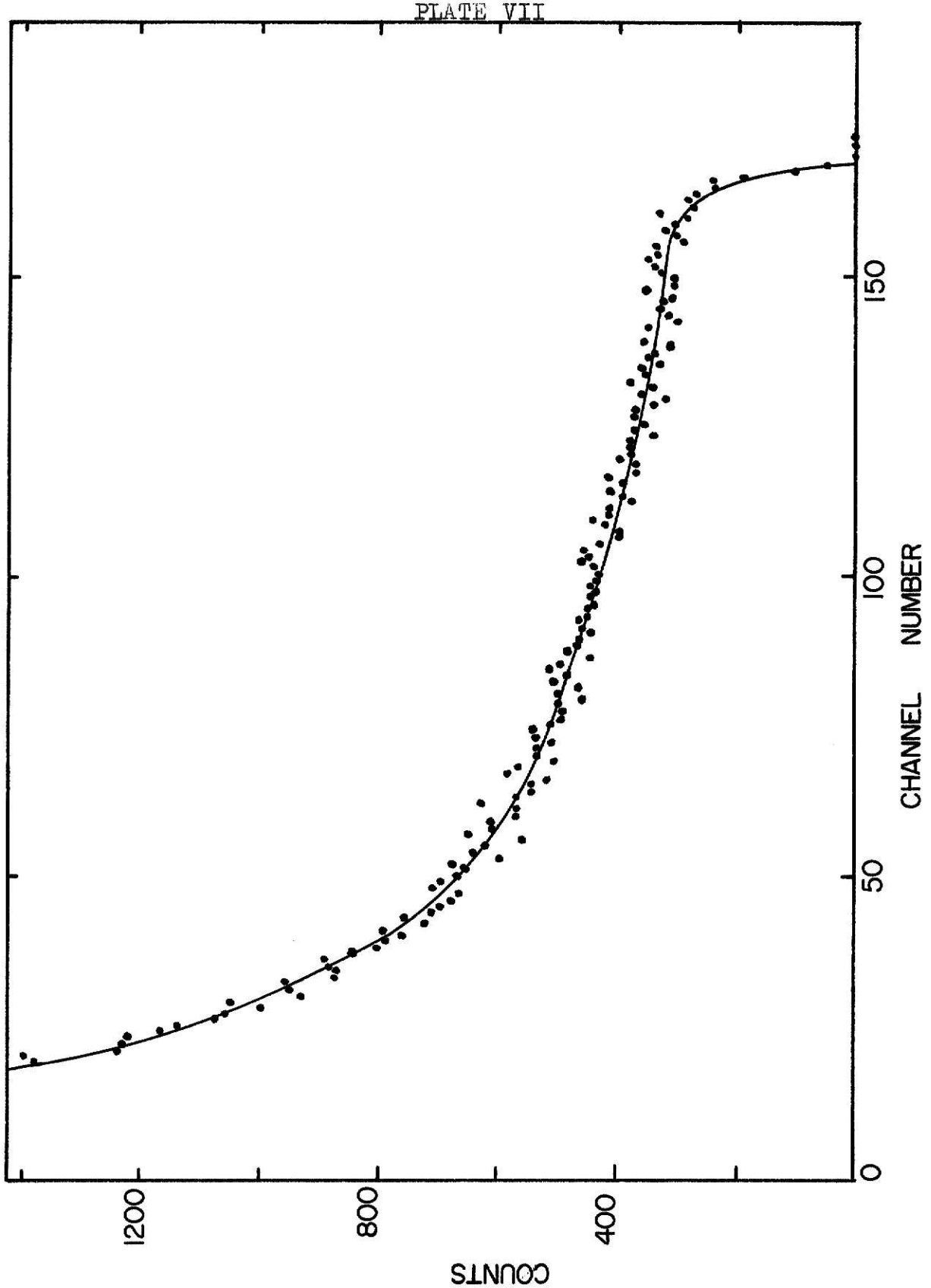

EXPLANATION OF PLATE VIII

Plate VIII Calibration curve for 24 MeV ^{16}O scattered into 170°.

PLATE VIII

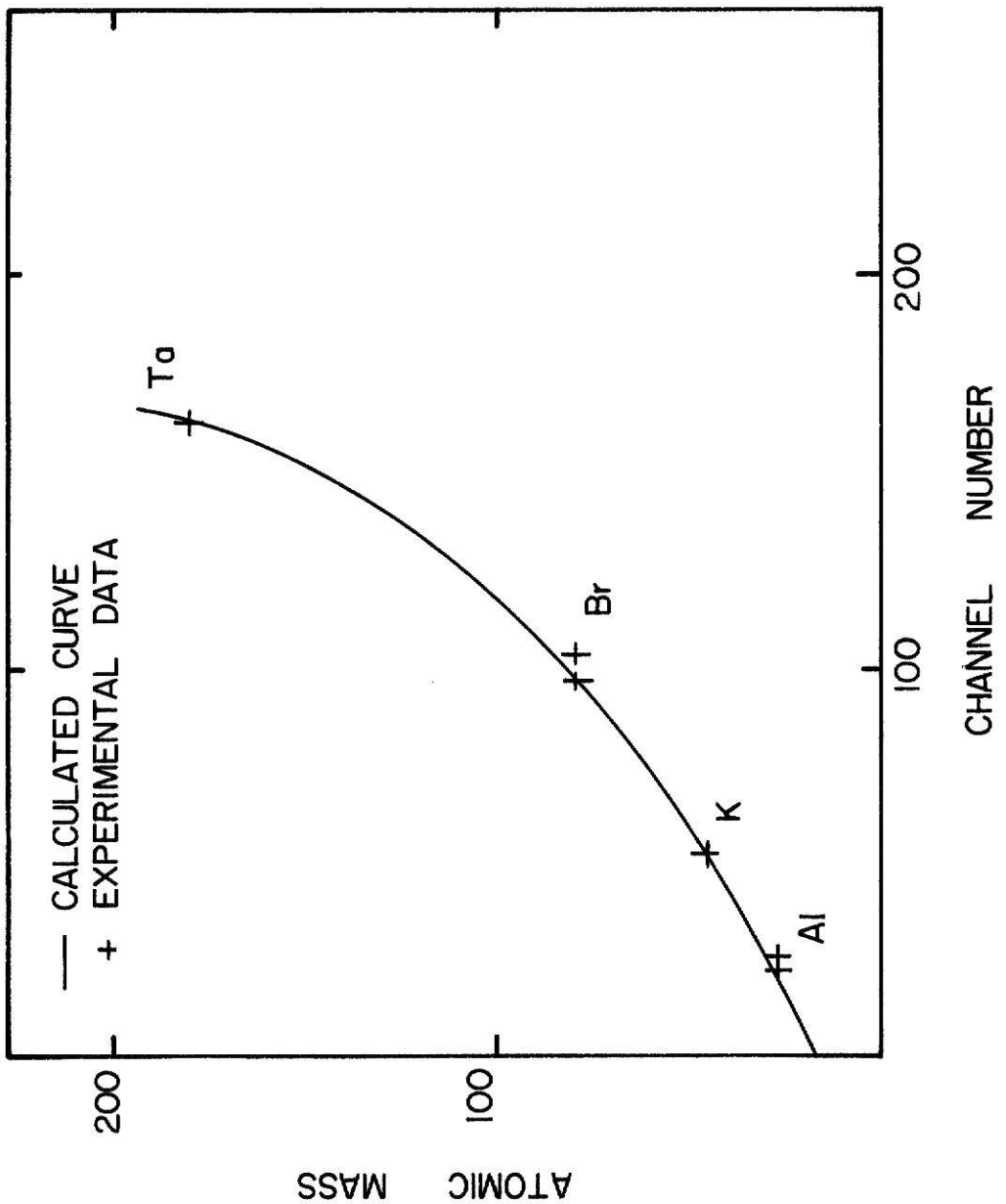
CALCULATED CURVE
+ EXPERIMENTAL DATA
Ta
Br
K
Al
200
100
ATOMIC MASS
100
200
CHANNEL NUMBER

EXPLANATION OF PLATE IX

Plate IX Spectrum of 24 MeV ^{16}O scattered into 170^{o} from 100 ppm $PbNO_3$ in flour.

PLATE IX

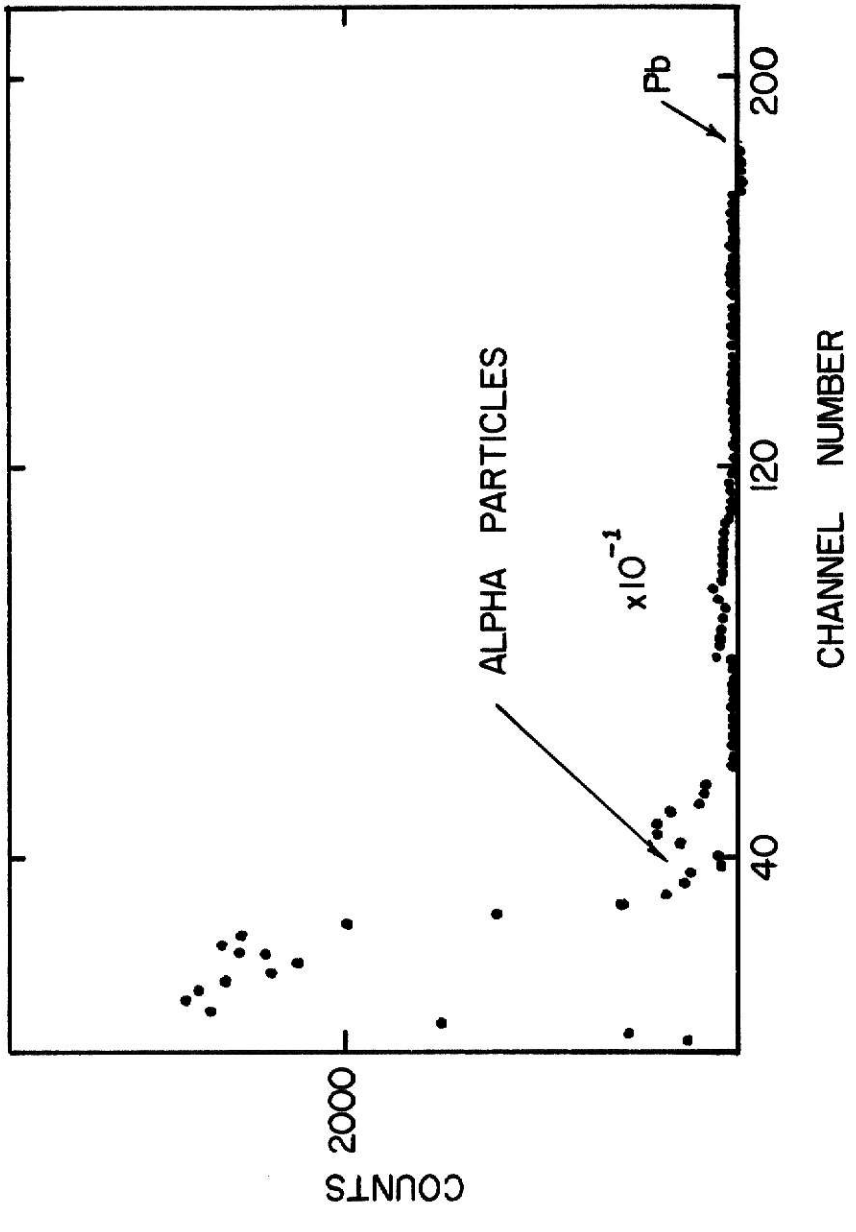
Pb
200
120
40
ALPHA PARTICLES
x10⁻¹
CHANNEL NUMBER
2000
COUNTS

EXPLANATION OF PLATE X

Plate X Spectrum of 12 MeV ^{16}O scattered into 170^{o} from 100 ppm $PbNO_3$ in flour.

PLATE X

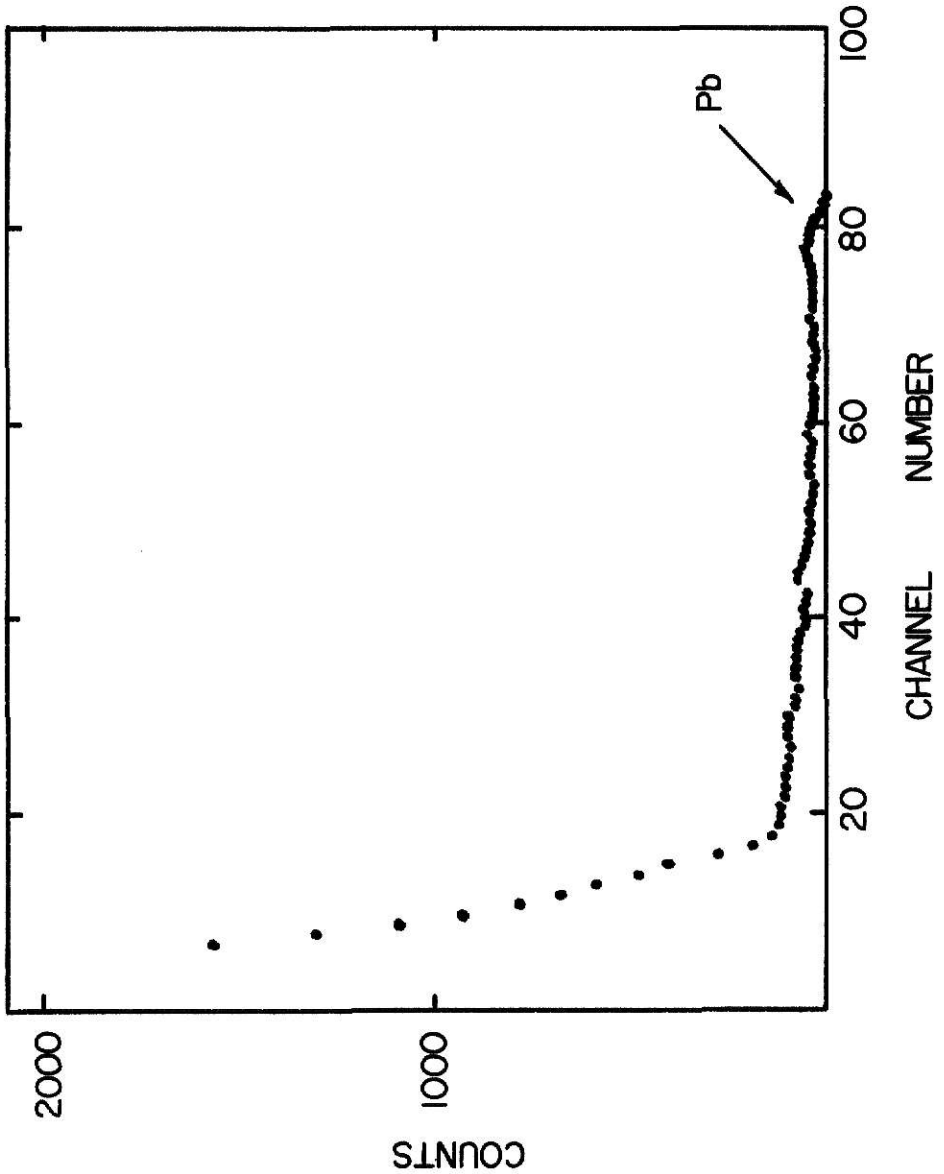

EXPLANATION OF PLATE XI a AND b

Plate XI Spectrum of 30 MeV ^{16}O scattered into 170^{o} from flour.

PLATE XIa

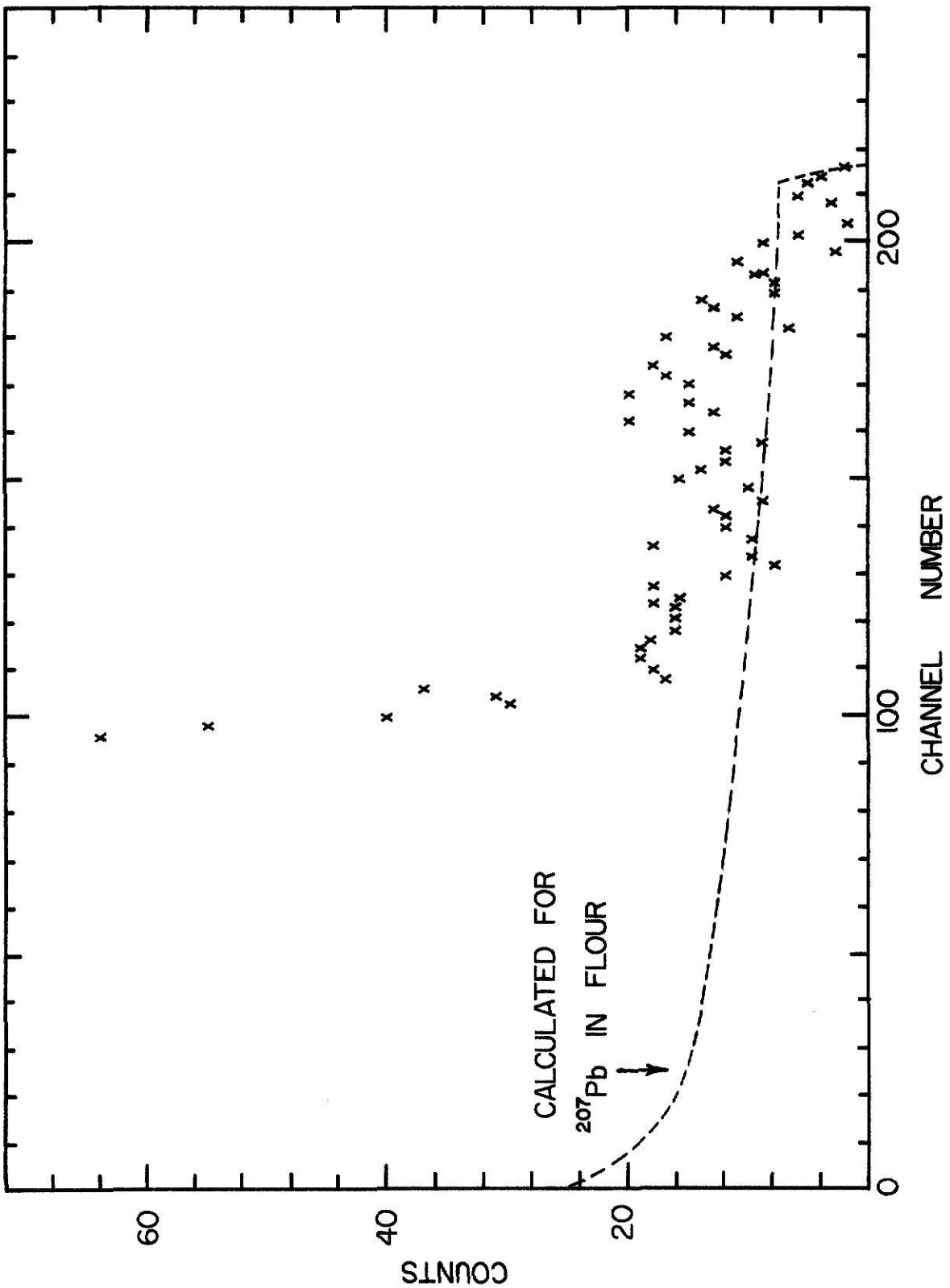
COUNTS
60
40
20
0
100
200
CHANNEL NUMBER
CALCULATED FOR
^{207}Pb IN FLOUR

PLATE XIb

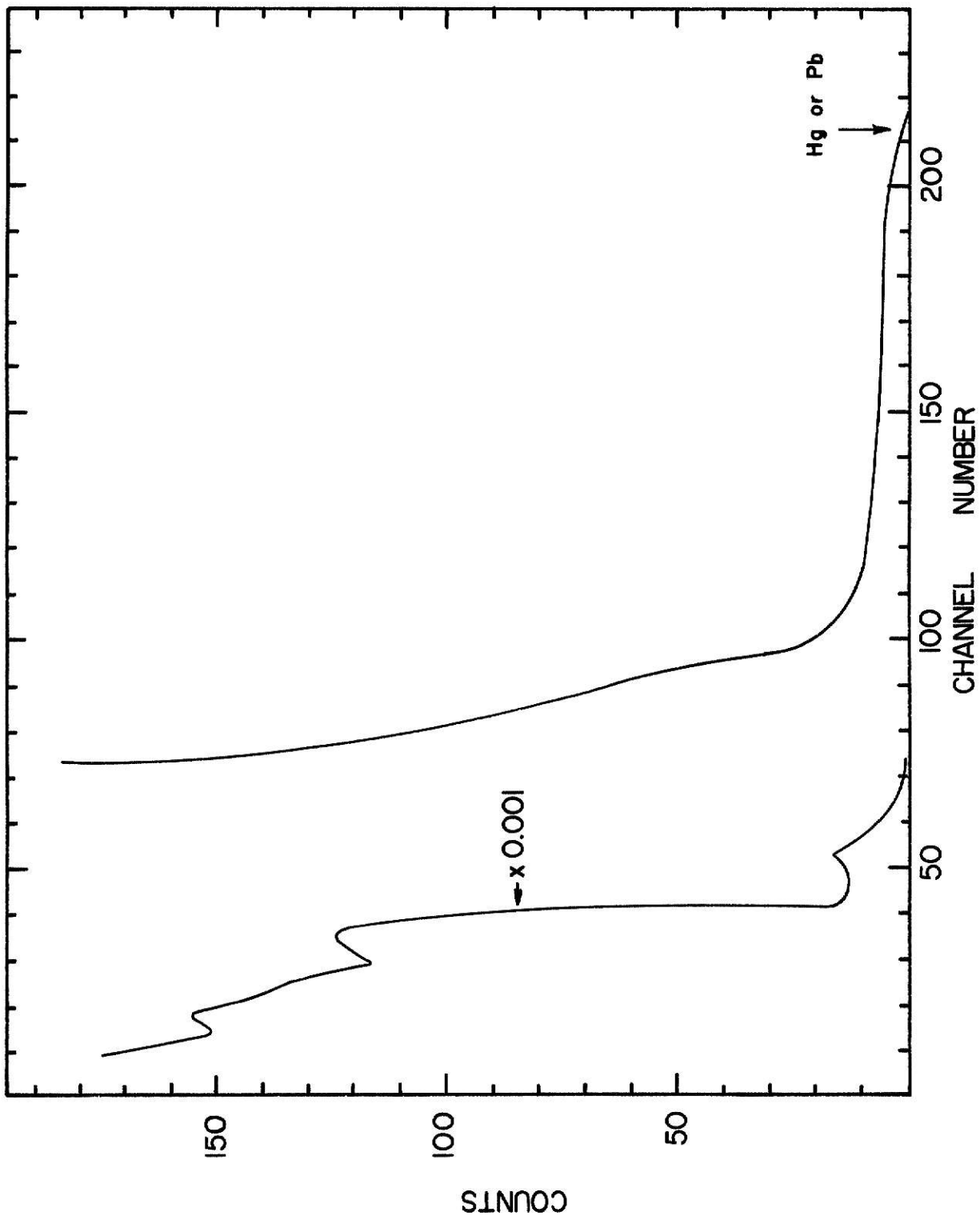

PREDICTED SPECTRA

It was found that spectrum shapes varied with target types and with energy. In order to determine which spectrum shape should be considered "good" and which spectrum shape should be "bad," a model spectrum was needed. A program code shown in plate XII was used to calculate the shape of the spectrum for elastic scattering from a thick target.

The program used the kinematics previously discussed and gave a value for the integrated yield from any one element considered as a contaminant. The integrated yield, Y_i, is proportional to the following integral, Y_p, the particle yield.

$$Y_p = \int Y dx \propto \int \frac{d\sigma}{d\Omega} \frac{dE}{dE/d(\varsigma x)} = Y_i$$

In addition to the above calculation, predicted spectra were obtained for comparison with experimental spectra. For each Δx or $\frac{dE}{dE/d(\varsigma x)}$ a value for $\frac{d\sigma}{d\Omega}$ was calculated. Thus the calculated spectra were generated as a graph of $\frac{d\sigma}{d\Omega}$ vs. x. Plate number XIII shows a predicted spectra for 24 MeV ^{16}O scattered into 170° from Br.

Plate XIa shows a predicted spectrum for 30 MeV ^{16}O scattered into 170° from ^{207}Pb. This spectrum shape also approximates the spectra obtained from 12 MeV ^{16}O scattered into 170° from 100 ppm $PbNO_3$ in flour.

In order to give a better representation, equal parts of sulfur, bromine, mercury, and lead were used to generate a predicted spectrum. Plate XIV shows this spectrum for 13 MeV ^{16}O

EXPLANATION OF PLATE XII

Plate XII The program code used to calculate the spectra shape for elastic scattering from a thick target.

PLATE XIIa

```
C       EIN = ENERGY INCIDENT
C       PROGRAM TO CALCULATE THE SPECTRUM SHAPE FOR ELASTIC
C       SCATTERING FROM A THICK TARGET.
C       DX/DS = INTEGER.GT.1, THETA IN DEGREES
C       DX,DS IN MG/CM**2, DEDS IN MEV/MG/CM**2
C       CONST IS A NUMBER TO SCALE THE CROSS SECTION VALUE, Y = CONST
      1*DSIG
        DIMENSION DEDS(100), EX(100), B(200), BB(200), NC(200)
        READ (1,2)(DEDS(K),K=1,100)
1       READ(1,2)EIN,A1,Z1,A2,Z2,THETA,DX,DS
        READ(1,2)CONST
2       FORMAT(8F10.5)
        DO 60 M = 1,200
        B(M) = 0.
60      BB(M) = 0.
        SUM = 0.0
        RAD = 180./3.1415926
        PSI = THETA/RAD
        DO 65 K = 1,100
65      EX(K) = FLOAT(K)
        WRITE(3,4)((EX(K+L-1),DEDS(K+L-1),K=1,100,20),L=1,20)
4       FORMAT(1H1,'DE/D(RHOX) IN MEV/(MG/CM**2) VS MEV'/1HO,7,'E',
      1'6X,'DEDS'/(1H , 5(F10.1,F10.3 )))
        WRITE (3,3) EIN,A1,Z1,A2,Z2,THETA,DX,DS
3       FORMAT (1HO, 'INITIAL ENERGY =' F6.1,' MEV',5X,'A1 =' F8.3,
      1 5X'Z1 =' F5.1,5X,'A2 =' F8.3,5X,'Z2 =' F5.1,5X, 'LAB ANGLE
      2 =' F6.1 / 1HO,'RANGE STEPS IN OVERALL CALC. OF F8.3, ' MG/
      3 (CM**2), RANGE STEPS IN DELTA E CALC. OF' F8.3, ' MG/(CM
      4 **2)'  )
        WRITE (3,5)
5       FORMAT (1HO,6X, 'X', 7X, 'DE1',6X, 'E1',6X, 'E3','DE2',6X,
      1 'EF',8X,'R',6X,'I',5X,'II',8X,'DISC',9X,'Y'
        WRITE (3,61)
61      FORMAT (1H)
C       SCALE EIN TO NCH, SC2 TO NCH = 100 MEV
        NCH = 100
        SCALE = FLOAT(NCH)/EIN
        SC2 = FLOAT (NCH)/100
        X = DX
10      CALL DELTA (EIN,X,DEDS,EX,DS,DE1)
        E1 = EIN - DE1
        CALL CROSS (E1,A1,Z1,A2,Z2,PSI,DSIG)
        CALL KINE (E1,A1,A2,PSI,E3)
        CALL DELTA (E3,X,DEDS,EX,DS,DE2)
        EF = E3 - DE2
        R = EF/EIN
        I = IFIX(EF*SCALE + 0.51)
        II = IFIX(EF*SC2 + 0.51)
        Y = DSIG*CONST
        SUM = SUM + Y*DX
        B(I) = Y*DX
```

PLATE XIIb

```
      BB(II) = Y*DX
      WRITE (3,90) X,DE1,E1,E3,DE2,EF,R,I,II,DSIG,Y
90    FORMAT (1H,F9.2,F9.2,F9.2,F9.2,F9.2,F9.2,F9.2, 16, 1PE15.3,
     1 1PE15.3 )
      IF (EF - 1.0) 200,200,100
100   X = X + DX
      GO TO 10
200   CONTINUE
      DO 210 J = 1,NCH
210   NC(J) = J
      WRITE (3,220) SUM
220   FORMAT (1HO, 'TOTAL YIELD =' 1PE15.3)
      WRITE (3,201)
201   FORMAT (1HO, 'CH. NO.' 3X, 'B' 8X 'BB')
      WRITE (3,202)((NC(K+L-1),B(K+L-1),BB(K+L-1),K=1,100,20),
     1 L=1,20)
202   FORMAT (1HO/ (1H,5(16, F8.3, F8.3 )))
      GO TO 1
      END

      SUBROUTINE KINE (E1,A1,A2,PSI,E3)
      IF (A1-A2) 20,10,10
10    WRITE (3,11)A1,A2
11    FORMAT (1H,'A1.CT.A2',2F8.3)
      E3 = 0.0
      GO TO 50
20    SN = SIN(PSI)
      S = A2/A1
      B = (COS(PSI) + SQRT(S*S-SN*SN))/(1. + S)
      E3 = E1*B*B
50    RETURN
      END

      SUBROUTINE CROSS (E1,A1,Z1,A2,Z2,PSI,DSIG)
      S = A1/A2
      EIP = E1/(1.+S)
      R = Z1*Z2/EIP
      Q = S*SIN(PSI)
      THETA = PSI + ATAN(Q/SQRT(1.-Q*Q))
      C = 1./SIN(THETA/2.)
      DSIG = 1.296*R*R*C**4
C     DSIG IN MB/STERAD
      RETURN
      END

      SUBROUTINE DELTA (E,X,DEDS,EX,DS,DS,DE)
      DIMENSION DEDS(100),ES(200)
C     DEDS IN MEV/(MG/CM**2)
      N = IFIX(X/DS+1.01)
      ES(1) = E
      DO 100 J = 2,N
```

PLATE XIIc

```
      DO 30 I = 2,100
      EEE = ES(J-1)-EX(I)
      IF (EEE) 10,20,30
20    Y = DEDS(I)
      GO TO 40
10    Y = DEDS(I-1)+EEE*(DEDS(I)-DEDS(I-1))/(EX(I)-EX(I-1))
      GO TO 40
30    CONTINUE
40    CONTINUE
      ES(J) = ES(J-1)-Y*DS
      ET = ES(J)
100   CONTINUE
      DE = E-ET
      RETURN
      END
```

EXPLANATION OF PLATE XIII

Plate XIII A predicted spectrum for ^{16}O scattered into 170^{o} from Br.

PLATE XIII

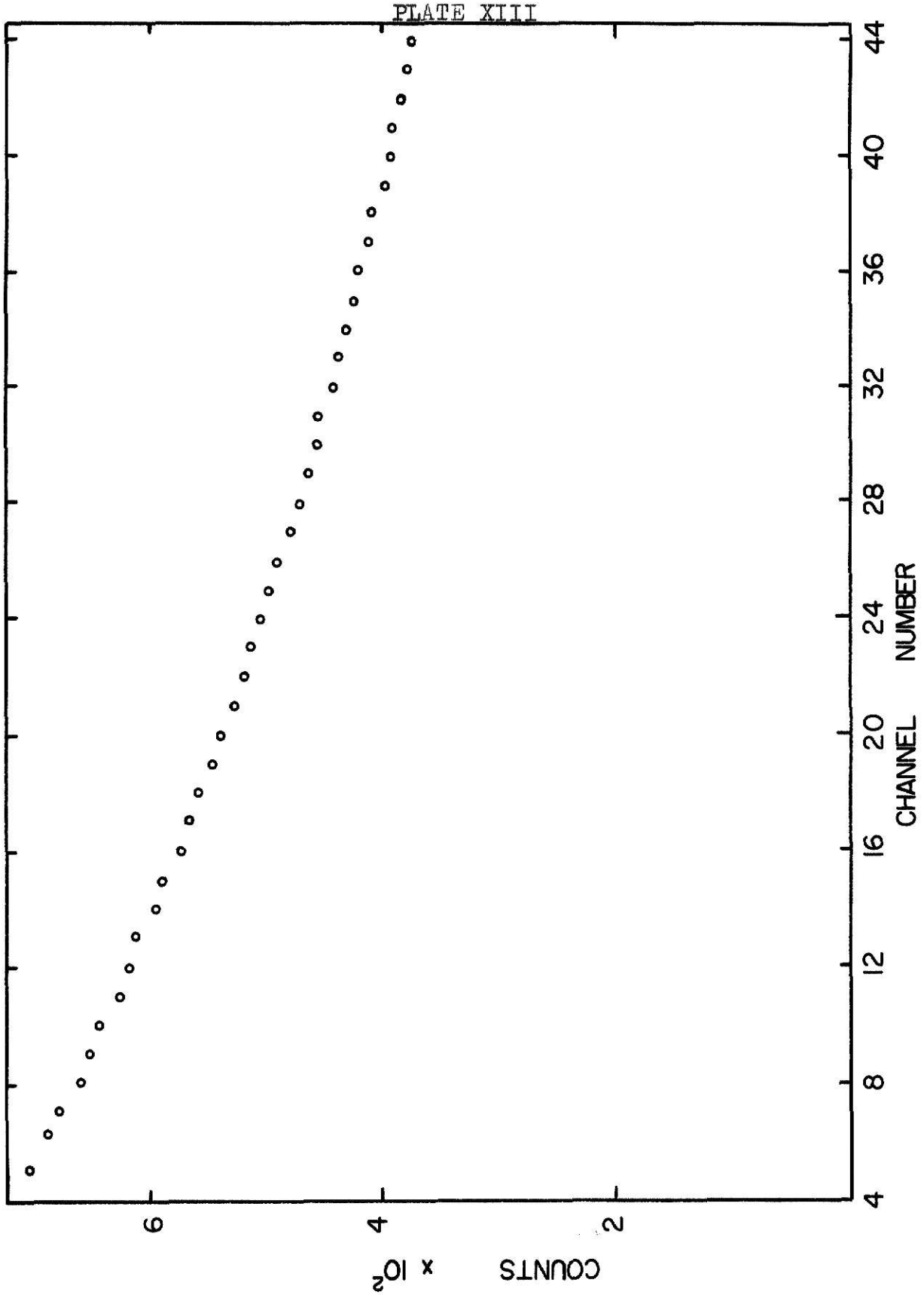

scattered into 90° from these four contaminants. By comparing this calculated spectrum with the spectra obtained from 12 MeV ^{16}O on $PbNO_3$ in flour, shown in plate X, it can be seen that the spectrum shapes are nearly identical.

By these comparisons it was felt that experimental spectra were predictable from the previously considered kinematical processes if and only if the incident ^{16}O energy, E_o, was 12 to 13 MeV. This was true for metal targets as well as flour targets.

In order to justify this assertion, a consideration of nuclear reactions was needed. There are several possible reactions to consider but one reaction was sufficient in predicting some spectrum energies.

EXPLANATION OF PLATE XIV

Plate XIV 13 MeV ^{16}O scattered into 90^{o} from equal parts of sulfur, bromine, mercury, and lead. The spectrum was calculated via a kinematic program for scattering from a thick target.

$Y_{Hg \ \& \ Pb} = 3.02 \times 10^{4}$ mg - mb/ster - cm^{2}

PLATE XIV

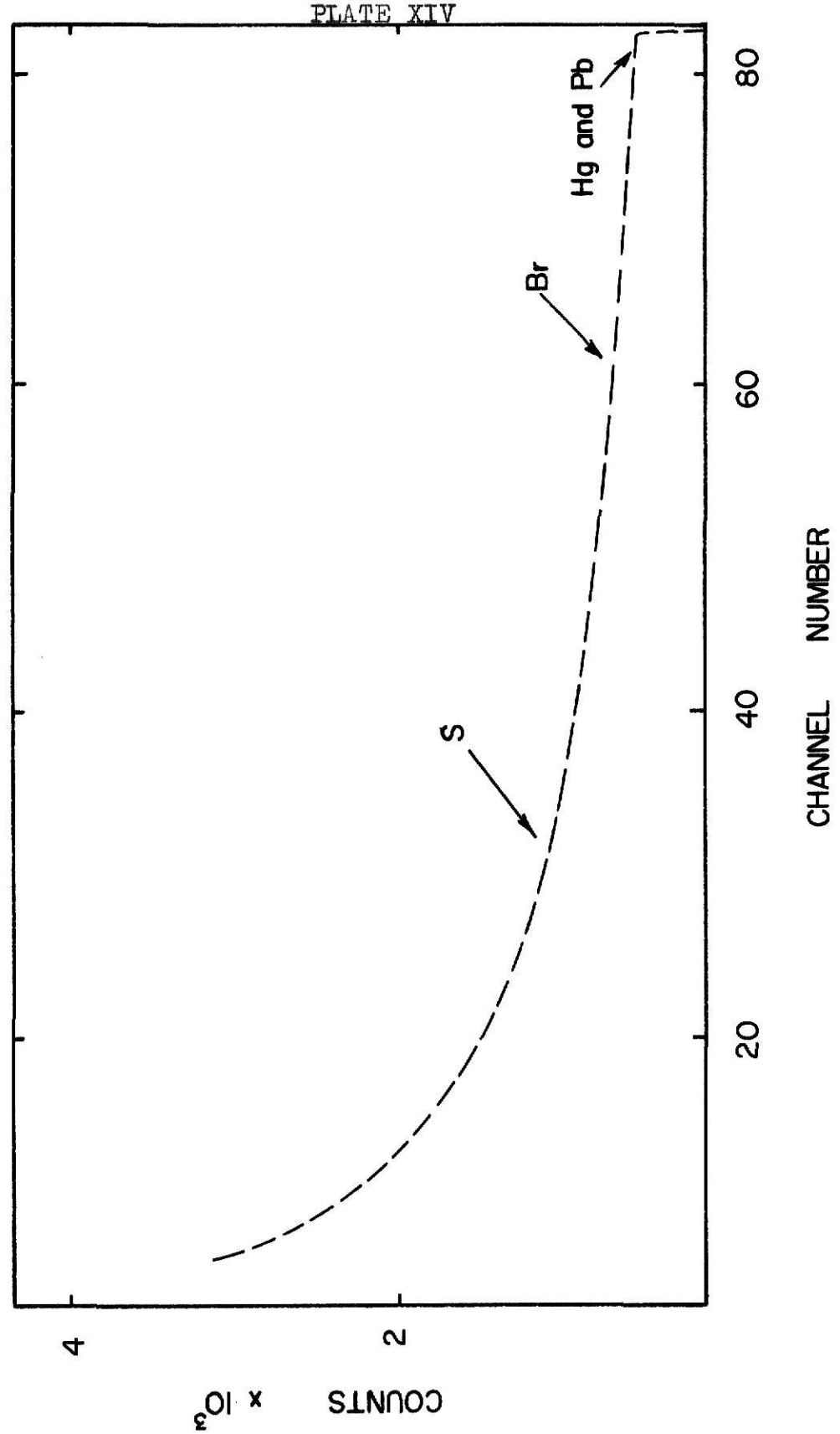

NUCLEAR REACTIONS

The probability of nuclear reactions is high when the energy of the incident particle is greater than the coulomb barrier. The energy of the coulomb barrier is given by the following formula.[10]

$$E_{CB} = \frac{Z_1 Z_2 e^2}{r_0 (A_1^{1/3} + A_2^{1/3})}$$

where Z_1 = atomic number of the incident particle

Z_2 = atomic number of the target

A_1 = mass number of the incident particle

A_2 = mass number of the target

$e^2 = 1.440 \times 10^{-13}$ MeV-cm

$r_0 = 1.2 \times 10^{-13}$cm

The coulomb barrier for $^{16}O\ (^{16}O, \alpha)^{28}Si$ is 15 MeV. Likewise, the coulomb barrier for $^{12}C\ (^{16}O, \alpha)^{24}Mg$ is 11.63 MeV. For energies that are above the coulomb barrier by a considerable amount, the spectrum can be expected to contain alpha particles or other products of nuclear reactions. In order to verify that nuclear reactions are prominent, spectra from 30 MeV ^{16}O scattered into 170° from flour were taken with the detector shielded from the oxygen ions by a sheet of aluminum foil. The aluminum foil allows alpha particles, protons, and gamma rays to be detected but the oxygen ions are stopped in the foil. This spectrum is shown in plate XV. If this spectrum is compared to the spectrum

---

10. Paul, op. cit., pp. 16-19.

with the flour target in plate IX, it can be seen that the spectrum shapes are very similar.

In order to calculate the maximum energy of the alpha particles consider the following reaction.

$$^{16}O + {}^{16}O \longrightarrow {}^{4}He + {}^{28}Si + Q$$

By use of mass tables the Q for the above reaction was calculated and found to be 9.599 MeV. Plate XVI shows a schematic of inelastic scattering theory with the laboratory formula for the energy of the particle M_3, the alpha particle. Plate XVII shows a table of alpha particle energies as a function of incident energy and scattering angle Ψ.

EXPLANATION OF PLATE XV

Plate XV A spectrum of 30 MeV ^{16}O scattered into 170^{o} from flour with the detector shielded with aluminum foil.

PLATE XV

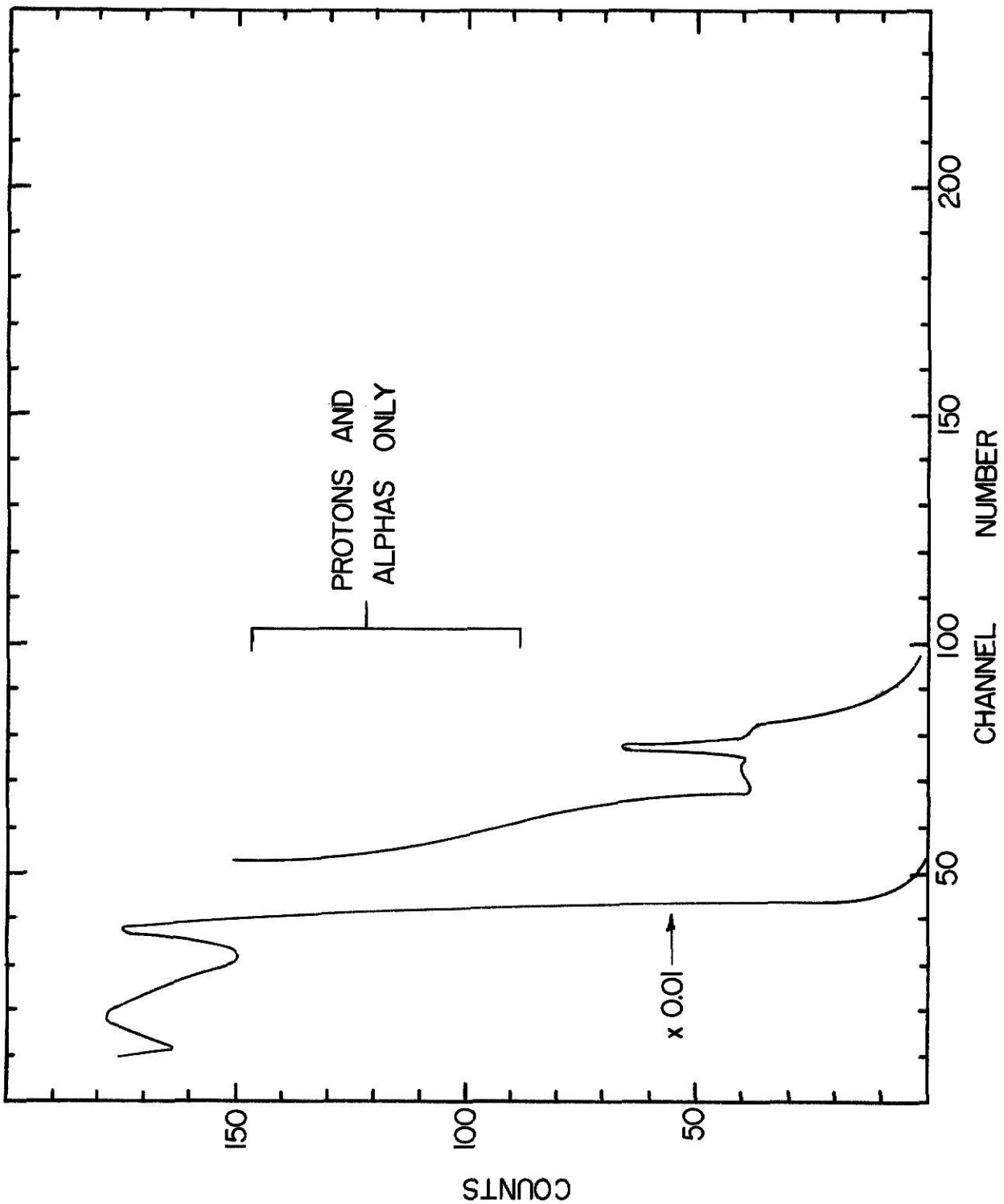
PROTONS AND
ALPHAS ONLY
x 0.01
COUNTS
150
100
50
50
100
150
200
CHANNEL NUMBER

EXPLANATION OF PLATE XVI

Plate XVI A schematic of inelastic scattering theory with formula for the energy of particle M_3 (the alpha particle) in the laboratory frame,

where

$$E_T = E_1 + Q = E_3 + E_4$$

$$E_3/E_T = B\,(\cos\Psi \pm (D/B - \sin^2\Psi)^{\frac{1}{2}})^2$$

where

$$B = M_1M_3(E_1/E_T)/(M_1 + M_2)(M_3 + M_4)$$

$$D = (M_2M_4/(M_1 + M_2)(M_3 + M_4))(1 + M_1Q/M_2E_T)$$

Ψ = laboratory scattering angle

PLATE XVI

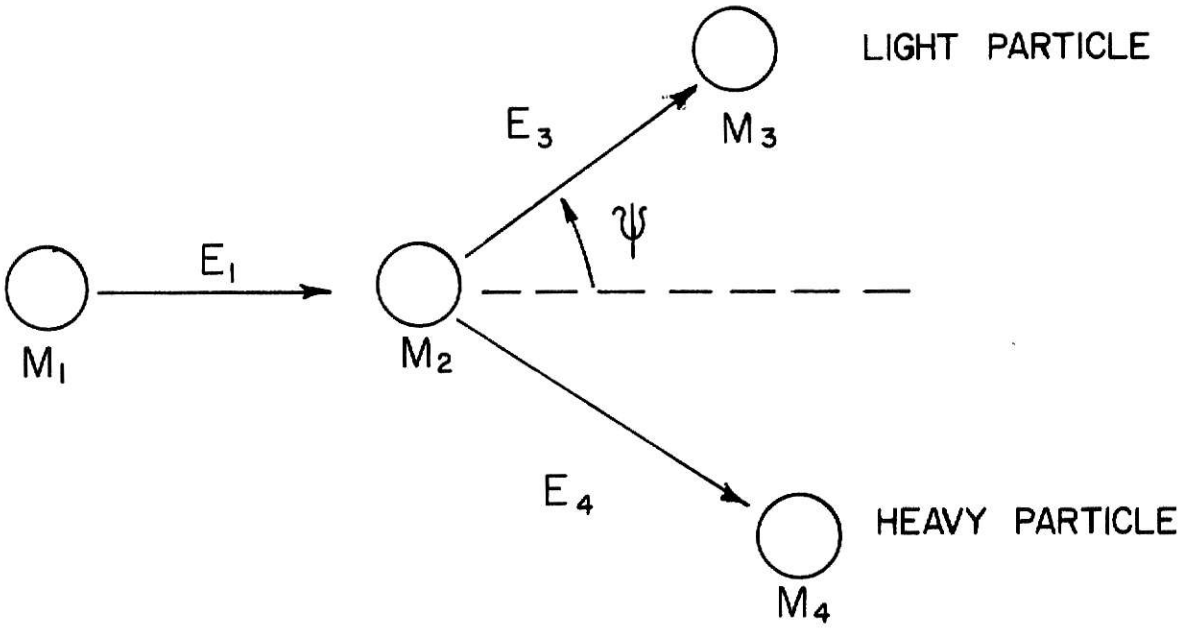

$$E_T \equiv E_1 + Q = E_3 + E_4$$

$$\frac{E_3}{E_T} = B \left[\cos \psi \pm \left({}^{D}/_{B} - \sin \psi \right)^{1/2} \right]^2$$

WHERE $$B = \frac{M_1 M_3 \left({}^{E_1}/_{E_T} \right)}{(M_1 + M_2)(M_3 + M_4)}$$

$$D = \frac{M_2 M_4}{(M_1 + M_2)(M_3 + M_4)} \left(1 + \frac{M Q}{M_2 E_T} \right)$$

ψ = LABORATORY ANGLE

EXPLANATION OF PLATE XVII

Plate XVII A table of alpha particle energies as a function of angle Ψ and incident energy E_1, where

$M_1 = {}^{16}O$

$M_2 = {}^{16}O$

M_3 = alpha particle

$M_4 = {}^{28}Si$

PLATE XVII

Ψ	E_1	E_3	E_3 / E_1
90°	30 MeV	19.7 MeV	0.656
90°	13 MeV	13.27 MeV	1.02
180°	30 MeV	10.69 MeV	0.3561
180°	24 MeV	8.12 MeV	0.3382

SPECTRA OBTAINED FROM 13 MEV ^{16}O IONS SCATTERED INTO 90^{o}

The 90^{o} spectra were taken as a second approach. This was primarily a time saving procedure. The time saving can be seen by considering a tantalum target. By calculating the ratio, $\frac{d\sigma(90^{o})}{d\sigma(180^{o})}$, for 13 MeV oxygen ions scattering from tantalum, the increase in particle yield would be the result. This ratio is equal to 3.27 and this implies a 327% increase in ^{16}O ion yield for 90^{o} scattering as compared to 180^{o} scattering. Also, the ratio E_3/E_1, is increased from 0.730 for 180^{o} scattering to 0.855 for 90^{o} scattering.

Tantalum was again used as the standard of calibration. Plate XVIII shows a typical tantalum spectrum. Once again a predicted curve fit was made to the tantalum energy edge. This fitted curve is shown in plate XIX. As can be seen, the curve fit is good; however, the discrimination between lead and mercury is poor. Notice also that the difference in the energy edges between lead and mercury is only two channels. As a result, either lead or mercury was **detected**, but discrimination between the two was impossible.

Plates XX through XXIII show representative spectra for 13 MeV ^{16}O on flour targets made from four different grains. They all have varying amounts of mercury or lead and possibly other trace elements.

For calibration of the ^{16}O yield, 100 ppm $HgNO_3$ in flour was used. Plate XXIII shows a spectrum for 13 MeV ^{16}O scattered into 90^{o} from 100 ppm $HgNO_3$ in flour. The ratio of the integrated

target current to the particle yield given by the spectrum is $(I/Y)_{100ppm}$. The concentration, D_1, in parts per ten thousand of the unknown sample is given by the following formula.

$$D_1 = (I/Y)_{100ppm} (Y/I)_{sample} (0.76) \text{ part per } 10^4$$

The factor, 0.76, is due to the ratio of atomic mass of mercury to the molecular mass of $HgNO_3$.

The method used to estimate the particle yield for lead or mercury from the flour spectra was based on the calculated lead and mercury spectrum. Plate XIV shows this spectra where the total number of particles for both lead and mercury were 3.02×10^4. Also, the spectrum area was approximated by a trapezoid. The spectrum height at channel number 45 times the total number of channels for both lead and mercury tends to approximate a trapezoidal area. The particle yield derived in this manner was 5.7×10^4 particles. This gives an error of thirty percent in the approximation of the particle yields.

Plate XXIV gives a tabulation of this analysis. As shown, small quantities of lead or mercury were detected in the eight flour samples. Smaller quantities could be detected by increasing the running time.

An interesting spectrum is that of flour sample #3 as shown in plate XXI. The spectrum shows a peak where the mercury edge should normally be. A peak such as that would result if the oxygen ions were scattered from a thin target. Therefore, it is logical to assume that there was a significant number of scattering centers of mass 200 on or near the surface of flour sample #3.

EXPLANATION OF PLATE XVIII

Plate XVIII A spectrum for 13 MeV ^{16}O scattered into 90^{o} from ^{181}Ta.

PLATE XVIII

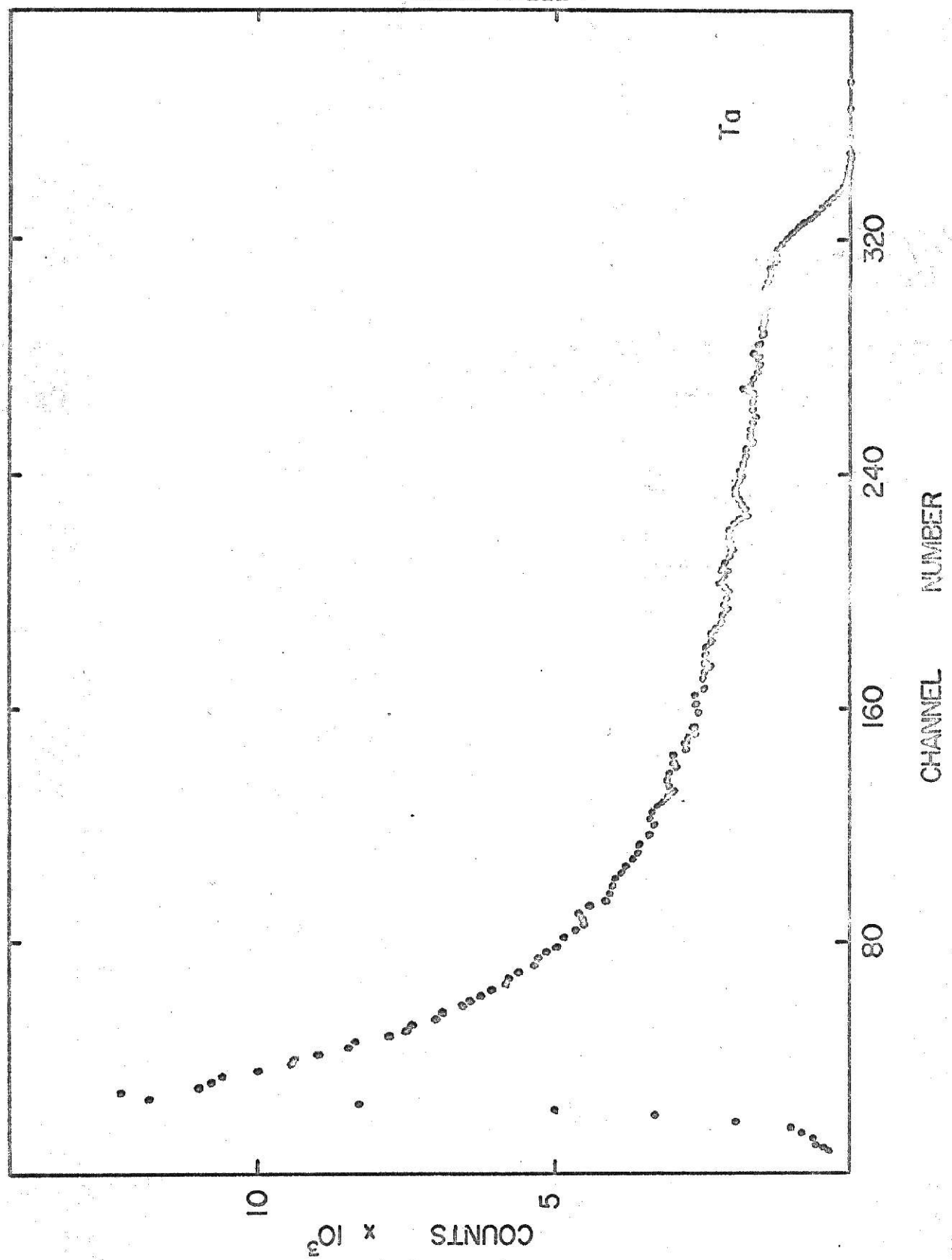

EXPLANATION OF PLATE XIX

Plate XIX A kinematic curve fitted to the tantalum energy edge for 13 MeV ^{16}O scattered into 90^{o}.

PLATE XIX

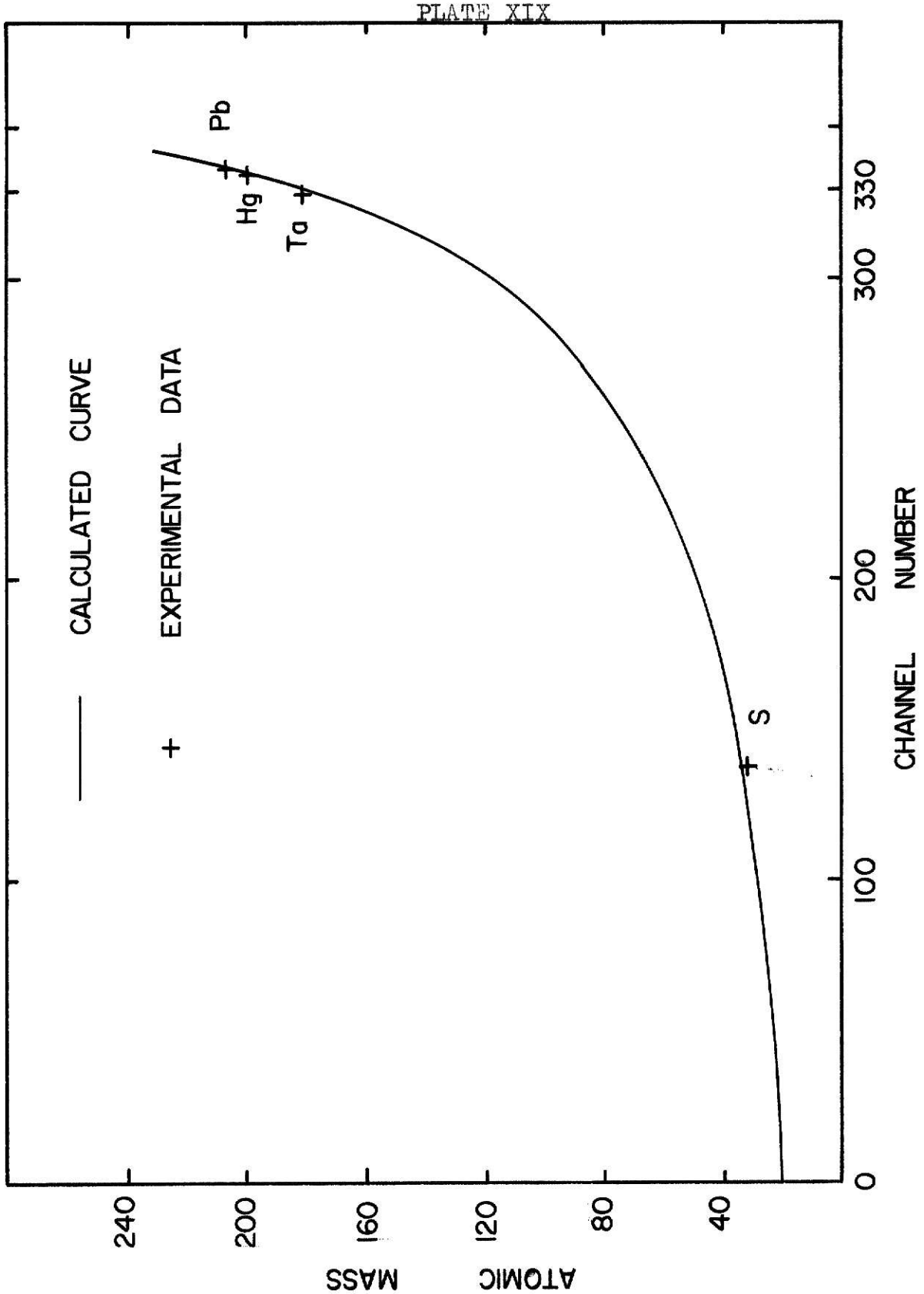
CALCULATED CURVE
EXPERIMENTAL DATA
Pb
Hg
Ta
S
ATOMIC MASS
240
200
160
120
80
40
0
100
200
300
330
CHANNEL NUMBER

EXPLANATION OF PLATE XX

Plate XX A spectrum for 13 MeV ^{16}O scattered into 90^{o} from flour sample #1.

I = 2.06×10^{5} counts

Y = 1.65×10^{5} particles

PLATE XX

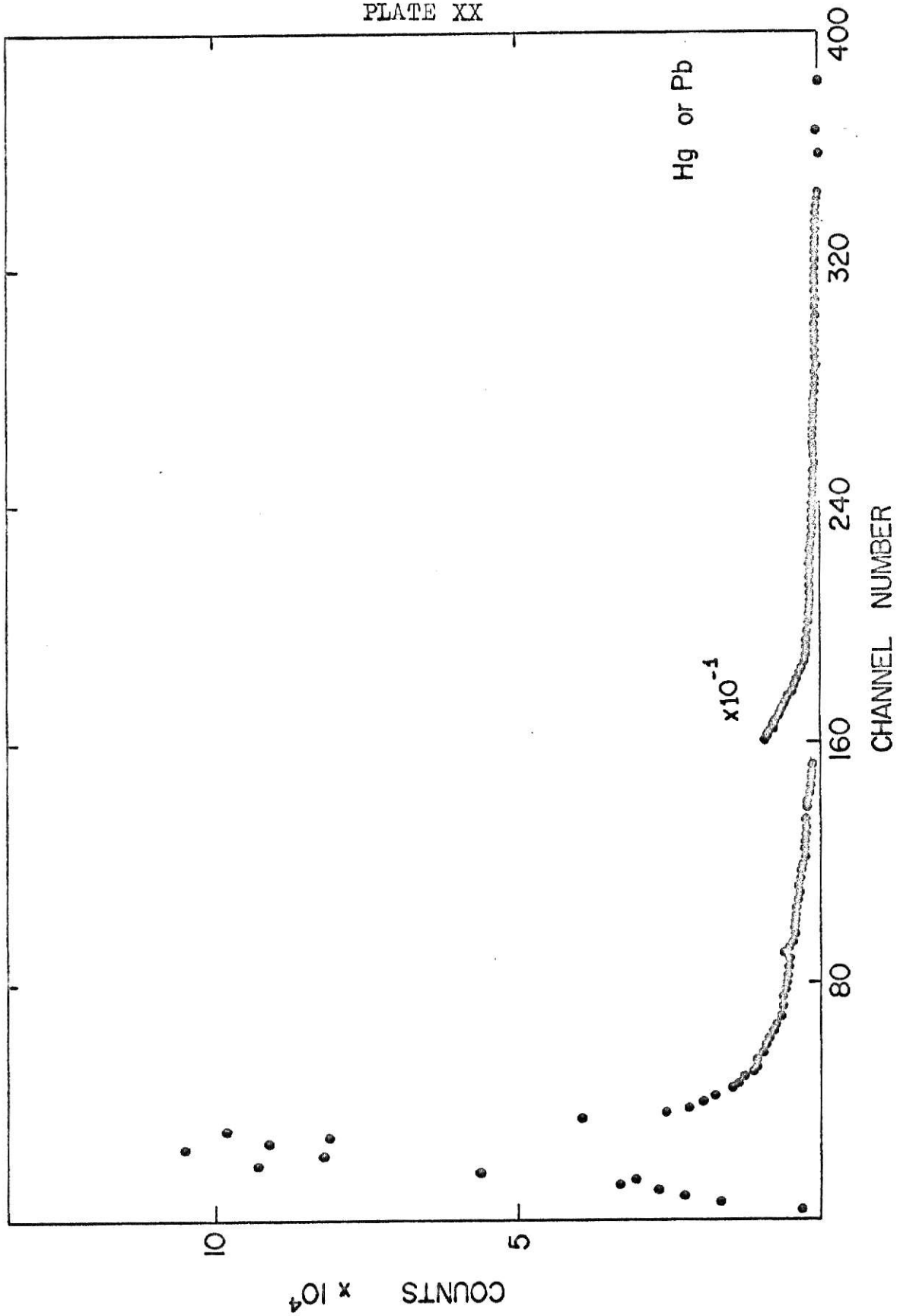
Hg or Pb
x10⁻¹
COUNTS x 10⁴
10
5
80
160
240
320
400
CHANNEL NUMBER

EXPLANATION OF PLATE XXI

Plate XXI A spectrum for 13 MeV ^{16}O scattered into 90^{o} from flour sample #3.

$I = 5.2 \times 10^{4}$ counts

$Y = 2.15 \times 10^{5}$ particles

PLATE XXI

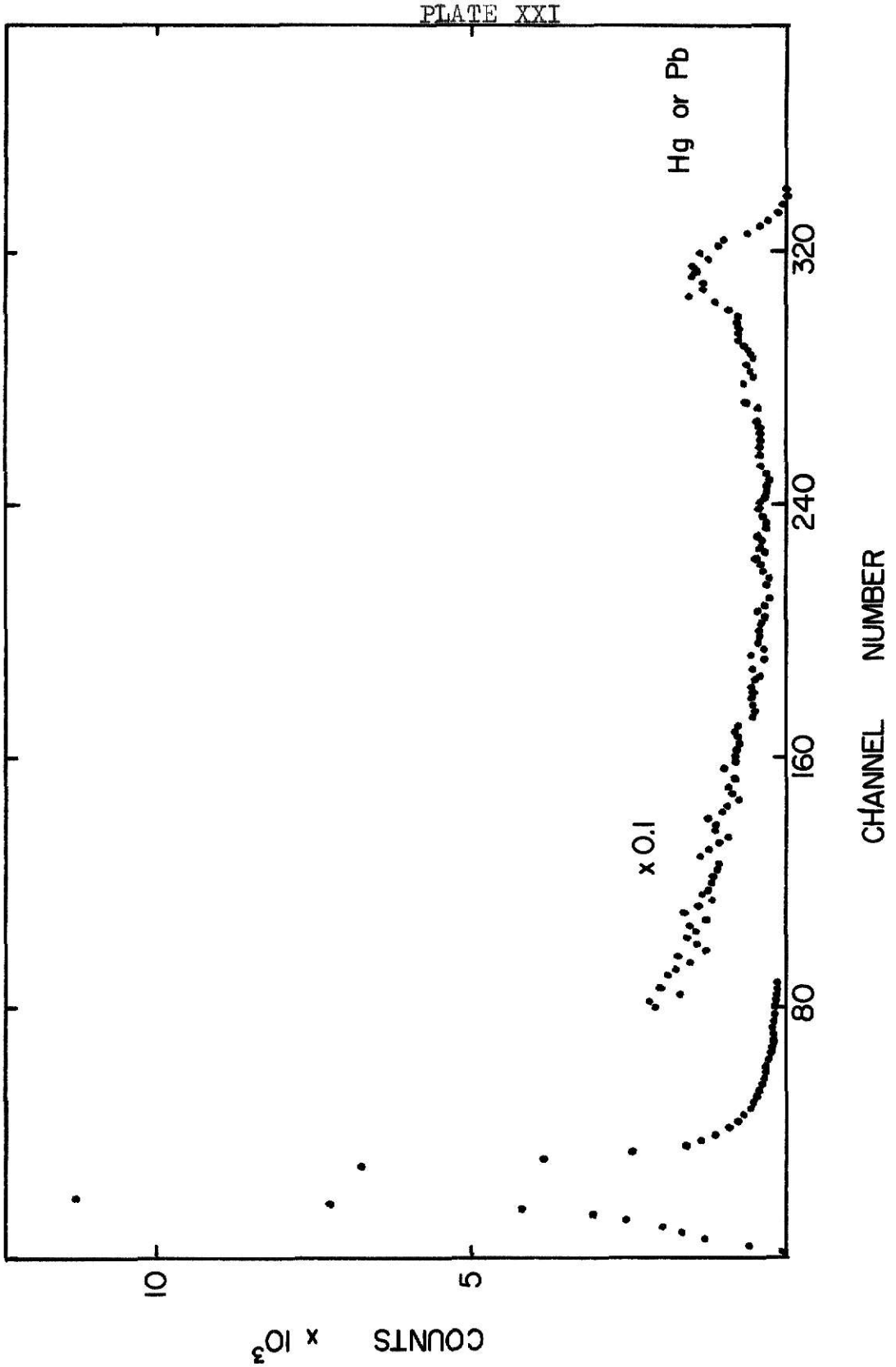

EXPLANATION OF PLATE XXII

Plate XXII A spectrum for 13 MeV ^{16}O scattered into 90^{o} from flour sample #4.

I = 8.19×10^{4} counts

Y = 4.46×10^{5} particles

PLATE XXII

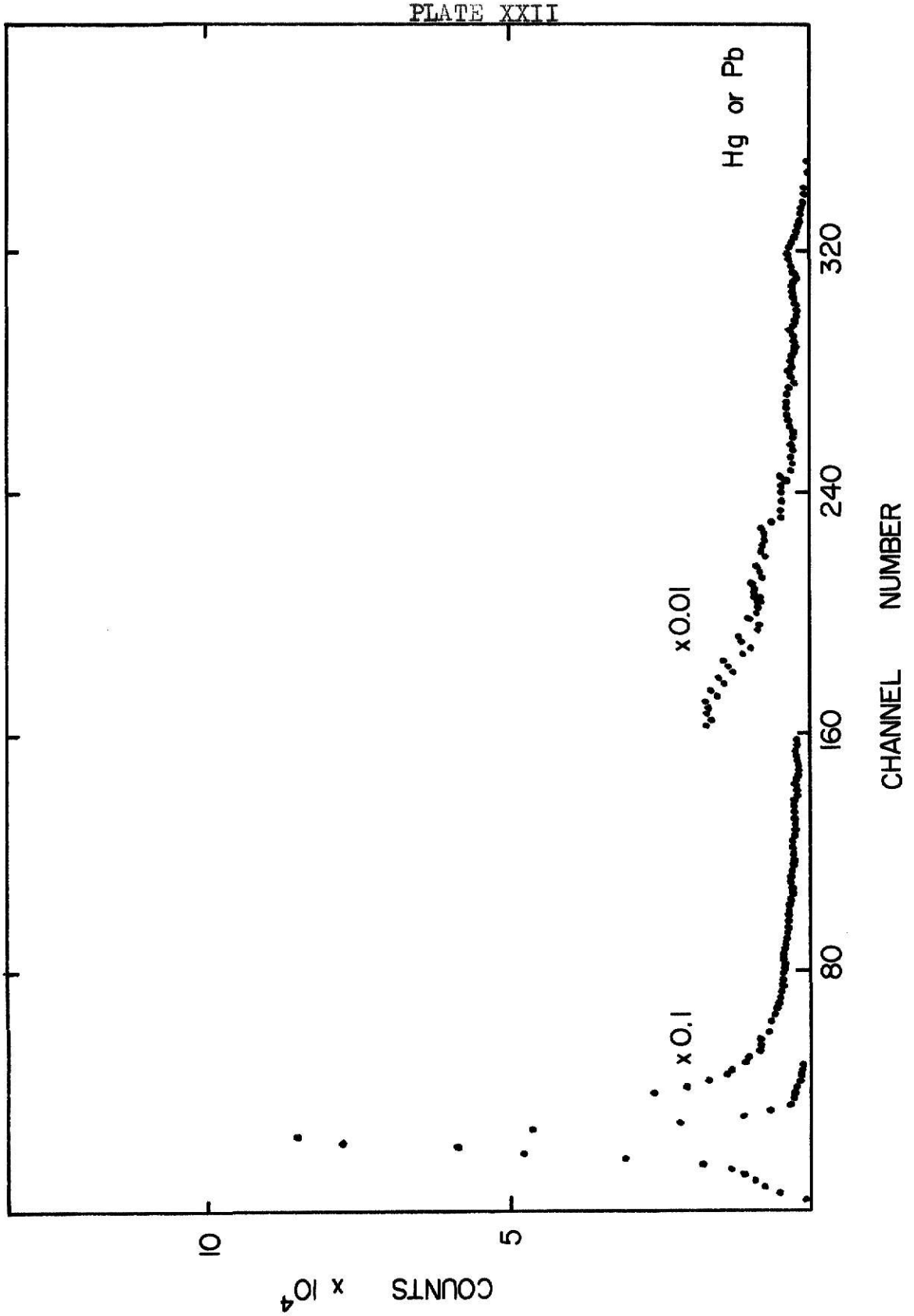
Hg or Pb
x0.01
x0.1
COUNTS x 10^4
10
5
80
160
240
320
CHANNEL NUMBER

EXPLANATION OF PLATE XXIII

Plate XXIII A spectrum for 13 MeV ^{16}O scattered into 90^{o} from 100 ppm $HgNO_3$ in flour.

I = 2.53×10^4 counts

Y = 1.15×10^5 particles

PLATE XXIII

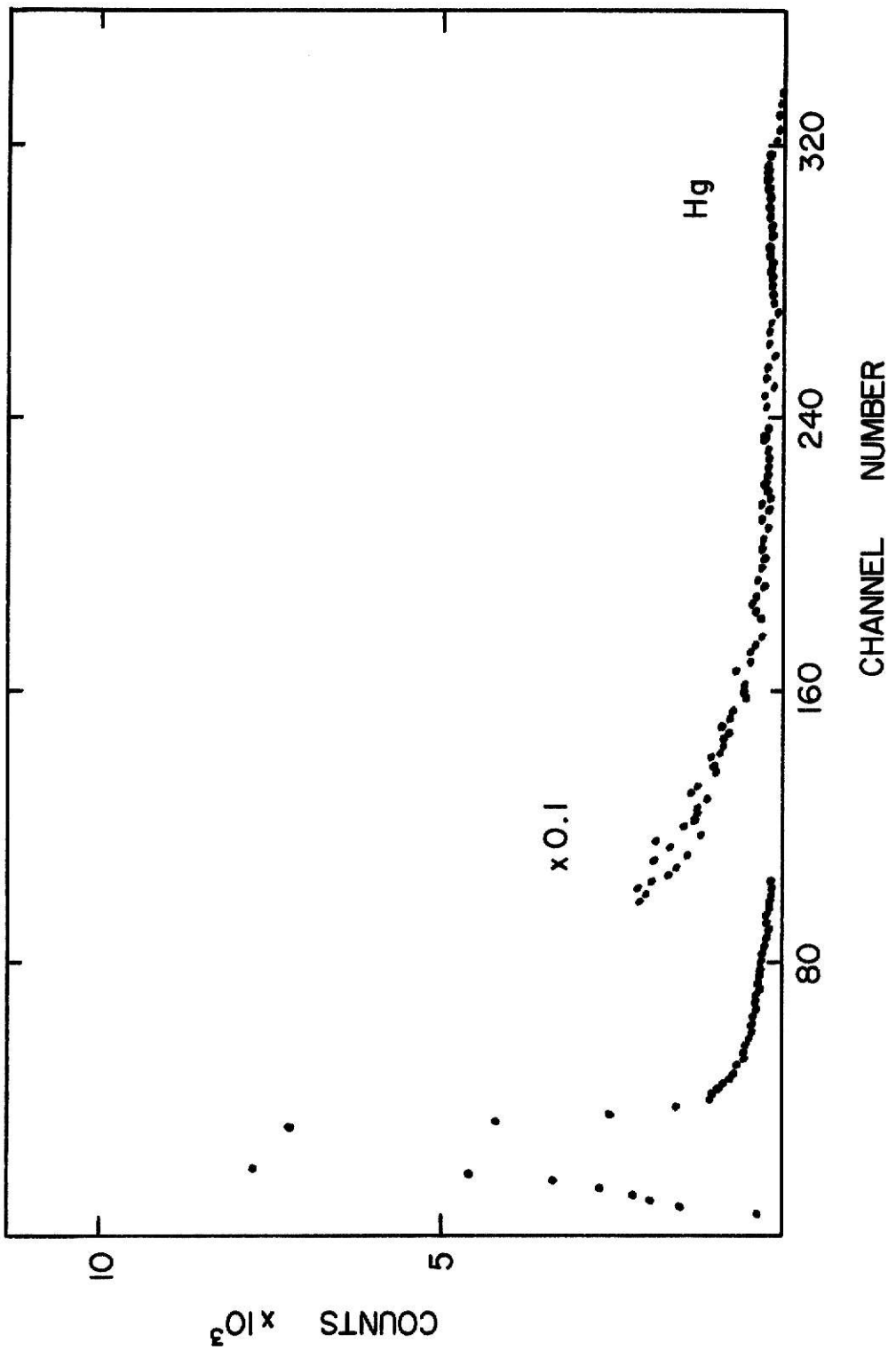

EXPLANATION OF PLATE XXIV

Plate XXIV A table of the concentration, D_1, for eight flour samples.

PLATE XXIV

Flour Sample	Y/I	D_1 (Hg or Pb) ± 30%
#1	0.801	13.4 ± 4
#2	2.065	34.5 ± 10
#3	4.14	69.1 ± 21
#4	5.45	91.0 ± 27
#5	2.98	49.7 ± 15
#6	2.26	37.8 ± 11
#7	3.205	53.5 ± 16
#8	1.39	23.2 ± 7

D_1 in parts per million

$(I/Y)_{100ppm}$ (.76) = 0.167

YIELD CALCULATIONS DERIVED FROM THE PREDICTED SPECTRA

The following section outlines the method used to calculate the concentrations of lead and mercury from predicted spectra. Plate XIV shows a calculated spectrum for lead, mercury, bromine, and sulfur. The program gave the following values for the integrated yield for each of the contaminants.

Contaminants	Integrated Yield in millibarns / steradian
Pb	1.56×10^4
Hg	1.46×10^4
Br	2.33×10^3
S	2.41×10^2

The following equation was stated previously.

$$\int Y \, dx = N_o \, n \, \Delta\Omega \int \frac{d\sigma}{d\Omega} \frac{dE}{dE} / d(\varsigma x)$$

It should be noted that n is the number of target atoms per centimeter squared. But, n is equal to the concentration, D, of the contaminant times Avagodro's number divided by the average atomic mass of the contaminant. By solving for the concentration, D_2, the following formula is obtained.

$$D_2 = \frac{\text{(spectrum yield) A}}{\text{(integrated yield)} \; \Delta \, \Omega \, N_o \, N_{AVAGODRO'S}}$$

Plate XXV shows the tabulated results for the kinematic calculations for the eight different flour samples. As a check for reliability between the concentration, D_1, and the concentration, D_2, the ratio, D_1/D_2, was taken for the eight flour samples. Plate XXV shows the results in the table. The values were

EXPLANATION OF PLATE XXV

Plate XXV A table showing example calculations of the concentration, D_2, for flour samples #1 through #8.

Flour Sample	Particle Yield	$\frac{\text{Particle Yield}}{\text{Integrated Yield}}$	$\left(\frac{3.29}{I}\right) \times 10^{-1}$	D_2(Hg or Pb)	$\frac{D_1}{D_2}$
#1	1.65×10^5	11.3	1.60×10^{-6}	18.1 ± 4	0.74
#2	1.65×10^5	11.3	4.11×10^{-6}	46.4 ± 11	0.74
#3	2.15×10^5	14.7	6.33×10^{-6}	93.0 ± 21	0.74
#4	4.46×10^5	30.5	4.02×10^{-6}	122.3 ± 28	0.74
#5	3.30×10^5	22.6	2.98×10^{-6}	67.6 ± 15	0.74
#6	1.98×10^5	13.6	3.76×10^{-6}	51.1 ± 12	0.74
#7	3.30×10^5	22.6	3.20×10^{-6}	72.4 ± 17	0.74
#8	1.48×10^5	10.1	3.10×10^{-6}	31.2 ± 7	0.74

D_2 and D_1 in parts per million

PLATE XXV

constant and D_1/D_2 was equal to 74%. Even though the absolute concentrations of lead and mercury are different, they have a direct correspondence. They differ only by a constant multiple that is not too far from being one.

ERROR CALCULATION

Northcliffe and Schilling state that their data is good to one percent at high energies for the stopping-power of heavy ions.[11] A reasonable error in the approximation of the stopping-power in flour is five percent. The largest contribution to error would occure in the measurement of the beam current on the target. An error of twenty percent is reasonable for the correction of the measurement of the electrons being scattered from the target. A third contribution to the error would be irregularities in the targets surface. Figure 2 shows a step irregularity of approximately 30 microns. Parallel paths of oxygen ions are shown with one being scattered and detected while the other was scattered and absorbed in the irregularity.

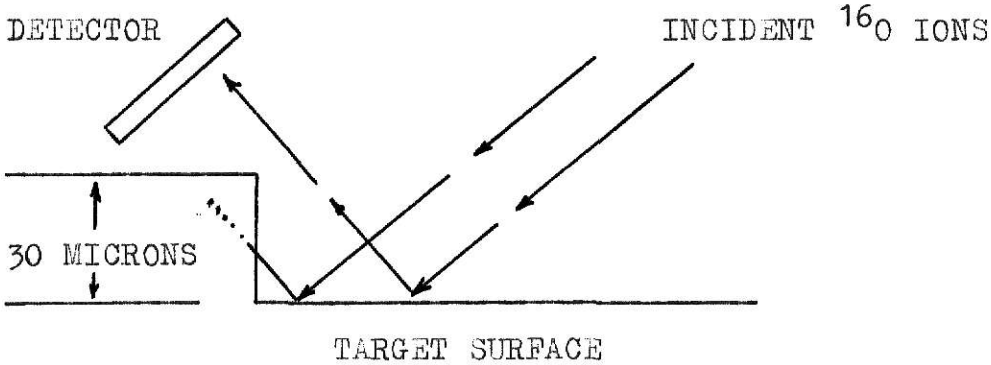

Fig. 2

An error of ten percent would also be a reasonable value for this situation. The error generated by the data taking process was small. The ADC consistantly registered one percent or less of the pulses lost due to dead time. Likewise, the solid angle of the

---

11. Northcliffe and Schilling, op. cit., p. 249.

detector was measured with an accuracy of better than one percent. The square root of the sum of the squares is twenty-three percent. This is a reasonable error for the calibration of the amount of lead or mercury in the flour samples by use of the predicted spectra.

It should be noted that in the previous two sections it was found that pure flour samples contained lead or mercury in amounts as great as one part in ten thousand. The flour samples used for calibration could have had as much as fifty percent more lead or mercury than the amounts added for calibration. This fact alone makes the above error estimate reasonable.

CONCLUSION

In concluding, the mass resolution must be considered, as well as some possible applications of this method. The mass resolution can best be seen on plate II. The ratio E_1/E_0 for nuclear masses 208 and 202 show a small but discernable difference. The ratio of E_1^{208}/E_1^{202} is 1.006 which shows the difficulty in differentiating between lead and mercury.

The resolution of the lead and mercury is poor but can be justified. The blurring of the edge is due to mercury's seven naturally occurring isotopes and the four of lead. Each isotope has a characteristic edge and would contribute to the total particle yield. These eleven different energy contributions would undoubtedly widen the edges for both lead and mercury.

A possible solution would be to observe the characteristic x-rays of lead or mercury while the runs are being made. This ratio along with the total concentration of both lead and mercury would give a clearer analysis.

This method should be useful on all biological samples that are clearly carbohydrates and proteins. This range of samples includes nearly all food stuff, both animal and vegetable. If lead and mercury could be resolved, it would be a valuable tool in the detection of contaminants in foods.

BIBLIOGRAPHY

Anonymous, "Proteins," The Encyclopedia Americana, 1949 Edition, XXII, pp. 676-679.

Ferris, Richard, "Carbohydrate," The Encyclopedia Americana, 1949 Edition, V, p. 587.

French, A.P., Principles of Modern Physics, New York, John Wiley and Sons, Inc., c. 1958.

Leighton, Robert B., Principles of Modern Physics, New York, McGraw-Hill Book Company, Inc., c. 1959.

Northcliffe, L.C., and R.F. Schilling, "Range and Stopping-Power Tables for Heavy Ions," Nuclear Data Tables, Academic Press, Inc., c. 1970.

Paul, E.B., Nuclear and Particle Physics, New York, American Elsevier Publishing Company, Inc., c. 1969.

ANALYSIS OF SURFACE COMPOSITION AND CONTAMINANTS IN BIOLOGICAL SAMPLES BY HEAVY ION SCATTERING

by

JON KENNETH WEST

B. S., Ottawa University, 1969

AN ABSTRACT OF A MASTER'S THESIS

submitted in partial fulfillment of the

requirements for the degree

MASTER OF SCIENCE

Department of Physics

KANSAS STATE UNIVERSITY
Manhattan, Kansas

1971

The Kansas State University Tandem Van de Graaff Accelerator has been used for detecting small amounts of lead and mercury in flour. The method involves a beam of oxygen ions incident on a sample of flour that is placed in a vacuum chamber. The energies of the scattered ions are measured and plotted. Beams of 12 to 30 MeV oxygen ions have been used, and the scattered ions were detected at angles of 165 to 175 degrees and 92 to 110 degrees with respect to the incident beam direction.

It was found experimentally that incident energy of the oxygen ion that was above the coulomb barrier gave unpredictable spectra.

This method is particularly useful for studying small concentrations of contaminants in biological samples. Biological samples are largely composed of elements no heavier than oxygen and so do not contribute to the spectrum.

The basis of the method is that an ion has greater final energy after scattering from a heavy atom than after scattering from a light ion. Thus, the scattered oxygen ion energy is greater from a sample of tantalum metal (atomic mass 181) than from a sample of aluminum foil (atomic mass 27). This energy difference is accentuated at the back angles of observation used. There is a continuous spectrum of final energies observed. This is because ions that penetrate into the sample lose some energy before and after scattering. Therefore, the energy at which the edge occurs is characteristic of the mass of the contaminant. Concentrations from 18 to 122 parts per million were found in the eight flour samples used in this study.